RESEARCH ARTICLE

Open Access

Juvenile stress induces behavioral change and affects perineuronal net formation in juvenile mice

Hiroshi Ueno[1,2*], Shunsuke Suemitsu[3], Shinji Murakami[3], Naoya Kitamura[3], Kenta Wani[3], Yosuke Matsumoto[4], Motoi Okamoto[2], Shozo Aoki[3] and Takeshi Ishihara[3]

Abstract

Background: Many neuropsychiatric disorders develop in early life. Although the mechanisms involved have not been elucidated, it is possible that functional abnormalities of parvalbumin-positive interneurons (PV neurons) are present. Several previous studies have shown that juvenile stress is implicated in the development of neuropsychiatric disorders. We aimed to clarify the effects of juvenile stress on behavior and on the central nervous system. We investigated behavioral abnormalities of chronically-stressed mice during juvenilehood and the effect of juvenile stress on PV neurons and WFA-positive perineuronal nets (PNNs), which are associated with vulnerability and plasticity in the mouse brain.

Results: Due to juvenile stress, mice showed neurodevelopmental disorder-like behavior. Juvenile stressed mice did not show depressive-like behaviors, but on the contrary, they showed increased activity and decreased anxiety-like behavior. In the central nervous system of juvenile stressed mice, the fluorescence intensity of WFA-positive PNNs decreased, which may signify increased vulnerability.

Conclusion: This study suggested that juvenile stressed mice showed behavioral abnormalities, resembling those seen in neuropsychiatric disorders, and increased brain vulnerability.

Keywords: Behavior, Juvenile, Mouse, Perineuronal nets, Parvalbumin, Stress

Background

Many neuropsychiatric disorders are diagnosed at puberty [1]. Approximately half of adult neuropsychiatric disorders begin in adolescence [2, 3]. However, the cause of the onset remains unclear. It has been reported that the onset of neuropsychiatric disorders such as anxiety, neurosis, depression, post-traumatic stress disorder (PTSD), and schizophrenia are associated with stress exposure during juvenilehood [4, 5]. In recent years, many children worldwide are experiencing stress [6]. Chronic stress is known as a major risk factor for the onset of numerous neuropsychiatric disorders including depression [7–9].

Human behavior is greatly affected by the environment both during childhood and adolescence [10–12]. The maturing brain is very sensitive to stress [13–15]. At this period, stressful events are related to later social and emotional maladjusted behaviors [16]. In animal experiment models, animals stressed in early childhood show increased anxiety-like behavior [17], decreased spatial memory [18], increased corticosterone secretion [19], and altered hippocampal size after maturation [18, 20].

Many common early-stage stress experiment models have focused on the period during lactation through maternal deprivation and separation. However, the development of the pup brain continues after weaning, and brain development is affected by environmental factors. In this study, we focused on mice after weaning. At this time, mice already act independently, and some areas of the central nervous system have matured, but many other

Ueno *et al. BMC Neurosci* (2018) 19:41

Page 2 of 21

brain areas have not [21–23]. Mice at postnatal week 4 are considered to be in the state before human juvenilehood, and their brain is still in the developmental stage [14]. Although the mechanisms involved in stress-related neuropsychiatric disorder development during juvenilehood and adolescence have not been elucidated, it seems that environment, physiology, and heredity are all implicated in a complicatedly interrelated manner [24]. Using animal experiment models, we are just beginning to understand how juvenile organs react to stress [25].

It has been suggested that functional abnormalities in parvalbumin-positive interneurons (PV neurons) are one cause of anxiety, neurosis, depression, and schizophrenia [26–32]. PV neurons are GABAergic interneurons [33–35]. In the central nervous system, GABAergic interneurons mature after birth, and abnormalities in GABAergic interneurons have been reported in numerous neuropsychiatric disorders [36–40]. PV neurons mature depending on environmental inputs around juvenilehood [41–43]. PV neurons form inhibitory synapses at the cell body and axon initial segments of pyramidal cells, and regulate the synchronous firing of pyramidal cells [44, 45]. Dysfunction of PV neurons causes mental disease-like behavior in mice [46, 47].

After birth, the cell bodies, proximal dendrites, and axon initial segments of many PV neurons are covered with special extracellular matrix molecules [48, 49]. This extracellular matrix molecules are called the perineuronal net (PNN). The PNN consists of hyaluronic acid, link proteins, tenascin, and aggrecan, versican, brevican, and neurocan, which are lecticans belonging to the family of chondroitin sulfate proteoglycans [50–53]. Lectin *Wisteria floribunda* agglutinin (WFA), which binds to *N*-acetylgalactosamine residues, is widely used to visualize PNNs [54]. Although the function of PNNs has not been clarified, it has been shown that they exert neuroplasticity control and have neuroprotective effects [55]. It is thought that the critical period ends by the formation of PNNs around PV neurons [56, 57]. Loss of PNNs around PV neurons restores plasticity, and reduces the excitability of PV neurons [58–60]. PNNs also protect PV neurons from oxidative stress [61, 62]. Altered PNNs have been reported postmortem in the brains of patients with schizophrenia and depression [63, 64], and mice with PNN dysfunction show behavioral abnormalities, such as those seen in neuropsychiatric disorders [65–67].

Behavioral abnormalities after maturation due to early life stress have been examined in detail, but behavioral anomalies in juvenilehoods under stress have not been clearly defined. If functional and structural anomalies are maintained until maturity, it is necessary to diagnose young people who are experiencing stress as soon as possible. Therefore, we aimed to clarify behavioral abnormalities in mice that had experienced stress during juvenilehood. In addition, we investigated the influence of stress on both PV neurons and PNNs in each brain region (frontal cortex, motor cortex, and the hippocampus) in juvenile mice.

The PV immunostaining-delineated CA2 neurons have not distinguishable differences in cell morphology compared with CA1 and CA3 regions. Hippocampal area CA2 is excluded from present study. Studies of neuropsychiatric disorders have implicated PV neuronal abnormalities in region-specific dysfunction and not in the sensory cortex. These reports indicate that there is region-specific vulnerability of PV neurons to neuropsychiatric conditions in the cortex. The motor cortex on the same section as the frontal cortex was examined simultaneously.

We physically and socially stressed mice for 10 days, which were at different developmental periods: early childhood (from postnatal day 21–30) and maturation phase (from postnatal day 81–90) on the same stress schedule. Therefore, in this study, we aimed to clarify the influence of stress on juvenile behaviors and on the formation of developing PV neurons and PNNs.

Methods

Animals

All animal experiments were performed in accordance with the U.S. National Institutes of Health (NIH) Guide for the Care and Use of Laboratory Animals (NIH Publication No. 80-23, revised in 1996) and were approved by the Committee for Animal Experiments at Kawasaki Medical School Advanced Research Center. All efforts were made to minimize the number of animals used and their suffering. The day of birth was designated as postnatal day (P0). Animals were purchased from Charles River Laboratories (Kanagawa, Japan) and housed in cages (5 animals/cage) with food and water provided ad libitum under a 12 h light/dark cycle at 23–26 °C. We used C57BL/6N male mice aged P21 (juvenile) and P71 (adult). Mice between the age of P0 and P28 are termed juvenile and mice between P28 and P56 should be termed adolescence. Since the adolescent period is quite ambiguity in rodents, we chose to start stress during what is considered to be the juvenile period (P21–30). Adult mice were exposed to stress from P71 to P80. The animals were randomly assigned to either the control (n = 10) or stress groups (n = 10). All behavioral tests were conducted in behavioral testing rooms between 08.00 and 18.00 h during the light phase of the circadian cycle. Similar to previous reports, we performed behavioral tests [68, 69]. After the tests, all equipment was cleaned with 70% ethanol and super hypochlorous water to prevent bias based on olfactory cues. Behavioral tests were performed two tests

Ueno *et al. BMC Neurosci* (2018) 19:41

Page 3 of 21

each day (Fig. 1). It takes 3 h between tests. Mice are back in their home cage in the colony.

Stress

Animals in the stress groups were subjected to stress once a day according to a protocol similar to that used in previous studies [70–73]. Animals were subjected to stress using the following procedures: (1) tail-pinch for 10 min; (2) forced restraint in a plastic tube for 3 h without access to food or water; (3) hot air (approx. 38 °C) blown using a hair dryer for 10 min; (4) overnight illumination; (5) food and water deprivation for 8 h; (6) damp sawdust (200 mL water absorbed in sawdust bedding). One stressor was applied daily (Fig. 1). Control mice were housed in a separate room, having no contact with the stressed mice.

General health and neurological screening

Physical characteristics, including body weight, rectal temperature, and presence of whiskers or bald hair patches, were recorded. The righting, whisker twitch, and ear twitch reflexes were also evaluated. Neuromuscular strength was examined using the grip strength and wire hang tests according to a previous study [74]. A grip strength meter was used to assess forelimb grip strength. Mice were lifted and held by the tail so that their forepaws could grasp a wire grid; they then were pulled backward gently until they released the grid. The peak force applied by the mouse forelimbs was recorded in Newtons (N). We performed this test at both P21 and P30.

Elevated plus maze test

The apparatus consisted of two open arms (8×25 cm) and two closed arms of the same size with 30-cm high transparent walls. The arms were constructed of white plastic plates and were elevated to a height of 40 cm above the floor. Arms of the same type were located opposite each other. Each mouse was placed in the central square of the maze, facing one of the closed arms, and was allowed to move freely between the two arms for 10 min. The number of arms entries, distance traveled (m), and percentage of time spent in the open arms were recorded on video and analyzed using video tracking software (ANY-MAZE, Stoelting Co., Wood Dale, IL).

Social interaction test

The apparatus consisted of a rectangular parallelepiped ($30 \times 60 \times 40$ cm). Each mouse was placed in the box for 10 min and allowed to freely explore for habituation. In the sociability test, an unfamiliar C57BL/6N male mouse (stranger mouse) that had no previous contact with the subject mouse was placed into one of the transparent cages ($7.5 \times 7.5 \times 10$ cm, which had several holes with a diameter of 1 cm) located at the corners of each lateral compartment. The stranger mouse was enclosed in the transparent cage, which allowed nose contact between the bars but prevented fighting. The subject mouse was placed in the center and allowed to explore the entire box for a 10-min session. One side of the rectangular area was identified as the stranger area and the other as the empty area. The amount of time spent in each area and around each cage during the 10-min sessions was measured. Data were recorded on video and analyzed using the ANY-MAZE software.

Porsolt forced swim test

The apparatus for the Porsolt forced swim test consisted of four Plexiglas cylinders (20 cm height $\times$ 10 cm diameter). The cylinders were filled with water (23 °C) up to a height of 7.5 cm. Mice were placed into the cylinders, and their behavior was recorded over a 6-min test period. In this test, we detect 'immobile period' when the animals stop struggling for one second or more. Immobility lasting for less than 1.5 s was not included in the analysis. Data acquisition and analysis were performed automatically using the ANY-MAZE software.

Tail suspension test

Each mouse was suspended 60 cm above the floor by the tail in a white plastic chamber by an adhesive tape placed < 1 cm from the tip of the tail. Its behavior was recorded for 6 min. Images were captured through a video camera, and immobility was measured. Similar to the Porsolt forced swim test, immobility was evaluated using the ANY-MAZE software.

Locomotor activity test

For measurements of locomotor activity, the mice were acclimated to the single housing environment for 2.5 h.

Fig. 1 Experimental time schedule. Animals in the stress groups were subjected to stress once a day from P21 (juvenile) or P71 (adult). Animals were subjected to two behavioral tests per day. *EPM* elevated plus maze, *PS* Porsolt forced swim, *YM* Y-maze, *TS* tail-suspension, *SI* social interaction, *LA* locomotor activity, *GHNS* general health and neurological screening

Ueno *et al. BMC Neurosci (2018) 19:41*

Page 4 of 21

Locomotor activity data were measured using a photo-beam activity system (ACTIMO-100; BRC Co., Nagoya, Aichi, Japan), and activity counts were recorded at 10-min intervals.

Y-maze test
Spatial working memory was measured using a Y-maze apparatus (arm length: 40 cm, arm bottom width: 3 cm, arm upper width: 10 cm, height of wall: 12 cm). Each subject was placed at the center of the Y-maze field. Visual cues were placed around the maze in the testing room and kept constant throughout the testing sessions. Mice were examined with no learning prior. The number of entries and alterations was recorded and analyzed automatically using the ANY-MAZE software. Data were collected for 10 min [75, 76].

Statistical analysis of behavioral tests
Data were analyzed with one-way analysis of variance (ANOVA) followed by Tukey's test, two-way repeated measures ANOVA followed by Fisher's LSD test, Student's t test, or paired t test. A p value < 0.05 was regarded as statistically significant. Data are shown as box plots.

Tissue preparation
Following behavioral experiments, we deeply anesthetized the animals with a lethal dose of sodium pentobarbital (120 mg/kg, i.p.) and transcardially perfused them with ice-cold phosphate-buffered saline (PBS) for 2 min and then 4% paraformaldehyde in PBS (pH 7.4) for 10 min (10 mL/min). In all cases, we dissected the brains and post-fixed them overnight with 4% paraformaldehyde in PBS at 4 °C and cryoprotected them by immersion in 15% sucrose for 12 h followed by 30% sucrose for 20 h at 4 °C. To cut sections, we froze the brains in O.C.T. Compound (Tissue-Tek; Sakuma Finetek, Tokyo, Japan) using dry ice-cold normal hexane and we prepared serial coronal sections of 40-μm thickness using a cryostat (CM3050S; Leica Wetzlar, Germany) at − 20 °C. We collected sections in ice-cold PBS containing 0.05% sodium azide.

Immunohistochemistry
The cryostat sections were treated with 0.1% triton X-100 in PBS for 15 min at 20 °C. After three washes in PBS, the sections were incubated with 10% normal donkey serum (ImmunoBioScience Co., WA) in PBS for 1 h at 20 °C. Sections were again washed three times in PBS and incubated with biotinylated WFA (B-1355, Vector Laboratories, Funakoshi Co., Tokyo, Japan; 1:200) and a primary antibodies in PBS overnight at 4 °C. After washing in PBS, the sections were incubated with streptavidin-conjugated to Alexa Fluor 594 (S11227, Thermo Fisher

Scientific, Tokyo, Japan; 1:1000) and secondary antibodies in PBS at 20 °C for 2 h. The sections were rinsed with PBS and mounted onto glass slides using Vectashield mounting medium (H-1400, Vector Laboratories). The prepared slides were stored at 4 °C until imaging.

Antibodies
The following primary antibodies were used: mouse anti-parvalbumin (clone PARV-19, P3088, Sigma-Aldrich Japan, Tokyo, Japan, 1:1000), mouse anti-NeuN (MAB377, Millipore, 1:1000), rabbit anti-Iba-1 (019-19741, Wako, Osaka, Japan, 1:1000), and mouse anti-Cat-315 (MAB1581, Millipore, Tokyo, Japan, 1:1000). The following secondary antibodies were used: Alexa Fluor 488-conjugated goat anti-mouse IgG (ab150113, Abcam, Tokyo, Japan; 1:1000), FITC-conjugated anti-mouse IgM (sc-2082, Santa Cruz, Texas, USA, 1:1000), and Texas Red-conjugated goat anti-rabbit IgG (TI-1000, Vector laboratories, 1:500).

Microscopic imaging and quantification of labeled neurons
To quantify the number of PV- WFA-, and Cat-315$^+$-positive neurons, confocal laser scanning microscopy of the stained sections was used according to a similar protocol [77]. Images (1024 × 1024 pixels) were saved as TIFF files using the ZEN software (Carl Zeiss Oberkochen, Germany). A 10 ×, or 20 × objective lens and a pinhole setting corresponding to a focal plane thickness of less than 1 μm were used. Data were quantified and presented according to the cortical layer profiles (L2/3 and L5/6) based on fluorescence Nissl staining (NeuroTrace 435/455 blue, N-21479, Molecular Probes, Eugene, OR). All confocal images were converted to TIFF files and analyzed with the Image J software (National Institutes of Health, Bethesda, MD; http://rsb.info.nih.gov/nih-image/). The number of neurons was quantified for at least three coronal sections per animal. The stained neurons or PNNs (defined as neurons with a soma size over 60 μm^2) were manually tagged and counted within the area of interest. Neuronal density estimates (cells/mm^2) were also calculated. The data were averaged per mouse. For analyzing PV-, WFA-, and Cat-315$^+$-positive PNN morphologies, samples were randomly selected, and high-magnification images using a 100 × objective lens were acquired.

Both fluorescent intensity and soma rea of PV neurons were quantified using at least three coronal sections per animal. Eight-bit grayscale images were captured using a digital camera. The ellipse circumscribing the PV-positive soma and WFA-positive PNNs was traced manually, and the gray levels for PV and WFA labeling were measured using the ImageJ software. We avoided fluorescence saturation by

Ueno *et al. BMC Neurosci* (2018) 19:41

Page 5 of 21

adjusting the exposure time and gain. The same capture conditions were used for all sections. Background intensity was subtracted using the unstained portions of each section. Data are presented as mean ± SEM. The slides were coded and quantified by a blinded independent observer.

Data analysis of histological quantifications

Data are expressed as the mean ± SEM of five animals per group. Statistical significance was determined by a two-way ANOVA followed by the Bonferroni t test. The statistical significance threshold was set at p < 0.05.

Results

Juvenile stress induces changes in body weight gain

We compared the general health and neurological characteristics of the juvenile-stressed and control groups. We found significant decreases in body weight and grip strength between juvenile-stressed and control group mice on P30 (Fig. 2a, stress × time: $F_{1,32} = 16.185$, p = 0.003; time in control: $F = 398.249$, p < 0.0001; time in stress group: $F = 219.906$, p < 0.0001; stress on P30: $F = 29.248$, p < 0.0001, Fig. 2c, stress × time: $F_{1,32} = 16.046$, p = 0.0003; time in control: $F = 51.697$, p < 0.0001; time in stress group: $F = 12.371$, p = 0.0013; stress on P30: $F = 21.798$, p = 0.0001). There were no significant differences in body temperature between
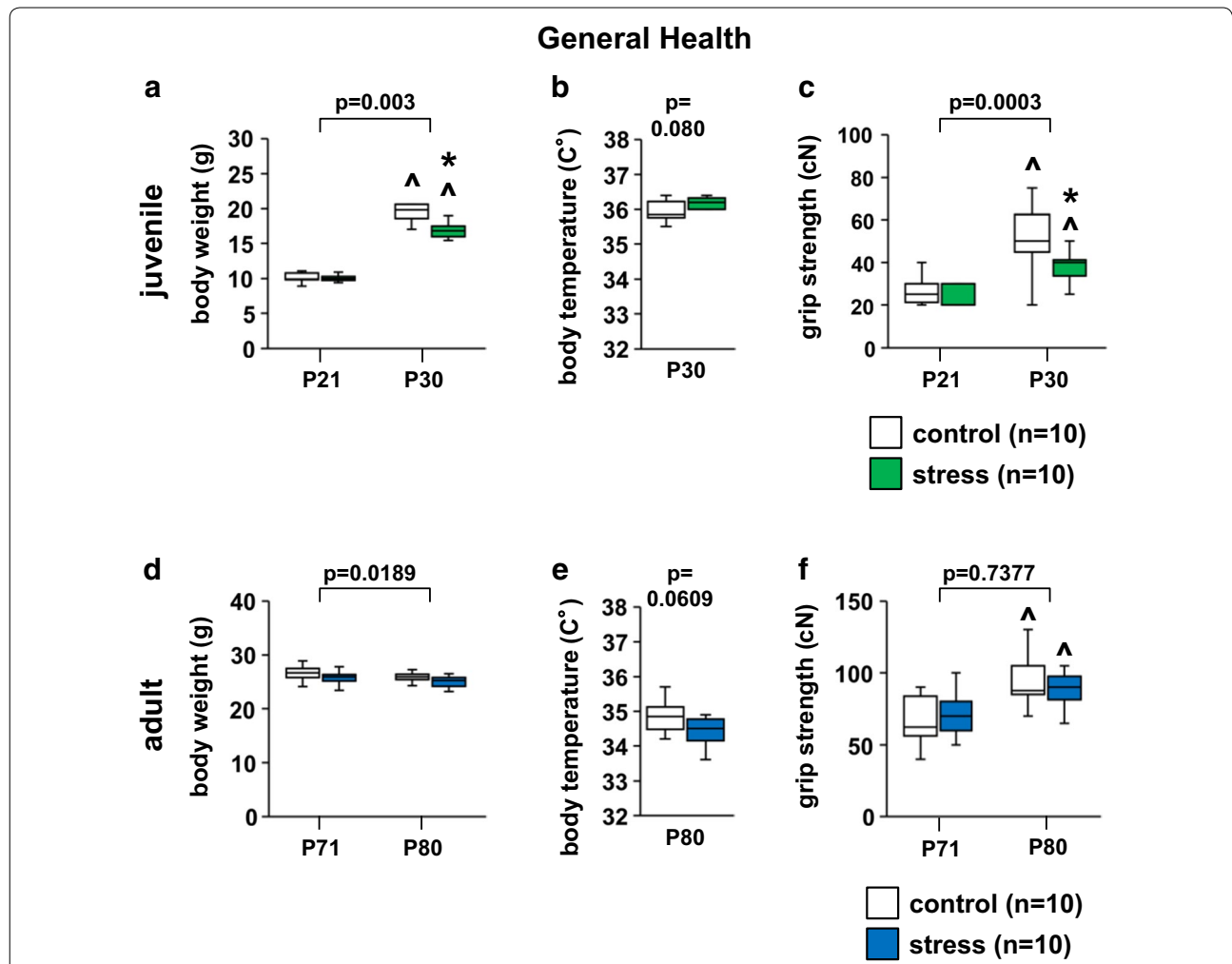
Fig. 2 Results of the general health and neurological screening in the stress and control groups. Juvenile: body weight before and after stress (**a**), body temperature (**b**), and grip strength before and after stress (**c**). Adult: body weight before and after stress (**d**), body temperature (**e**), and grip strength before and after stress (**f**). All data are presented as box plots. *Significant difference from control mice (p < 0.05). ^p < 0.05 versus first block; *p < 0.05 between time-matched stress and control groups. The p values were calculated by two-way repeated measures ANOVA (**a**, **c**, **d**, **f**) and Student's t test (**b**, **e**)

juvenile-stressed and control group mice on P30 (Fig. 2b, $t_{14} = 2.1448$, p = 0.080).

There were no significant differences in body weight, body temperature, and grip strength between adult-stressed and control group mice on P80 (Fig. 2d, stress × time: $F_{1,36} = 6.046$, p = 0.0189; time in control: $F = 1.303$, p = 0.2613; time in stress group: $F = 1.886$, p = 0.1782; stress on P80: $F = 3.440$, p = 0.0719, Fig. 2e, $t_{18} = 2.1009$, p = 0.0609; Fig. 2f, stress × time: $F_{1,36} = 0.114$, p = 0.7377; time in control: $F = 14.059$, p = 0.0006; time in stress group: $F = 4.183$, p = 0.0482; stress on P80: $F = 1.190$, p = 0.2826).

Juvenile stress did not change anxiety-like behaviors

We evaluated anxiety-like behavior in juvenile stressed mice. In the elevated plus maze test, we observed a significant increase in the total distance traveled in the juvenile-stressed compared with the control group mice (Fig. 3a, $t_{18} = 2.1009$, p = 0.0344). There were no significant differences in the number of total entries into the arms, and the percentage of time spent in the open arms between the juvenile-stressed and control group mice (Fig. 3b, $t_{18} = 2.1009$, p = 0.4545; Fig. 3c, $t_{18} = 2.1009$, p = 0.6605).

Next, we evaluated anxiety-like behavior in adult stressed mice. there were no significant differences in
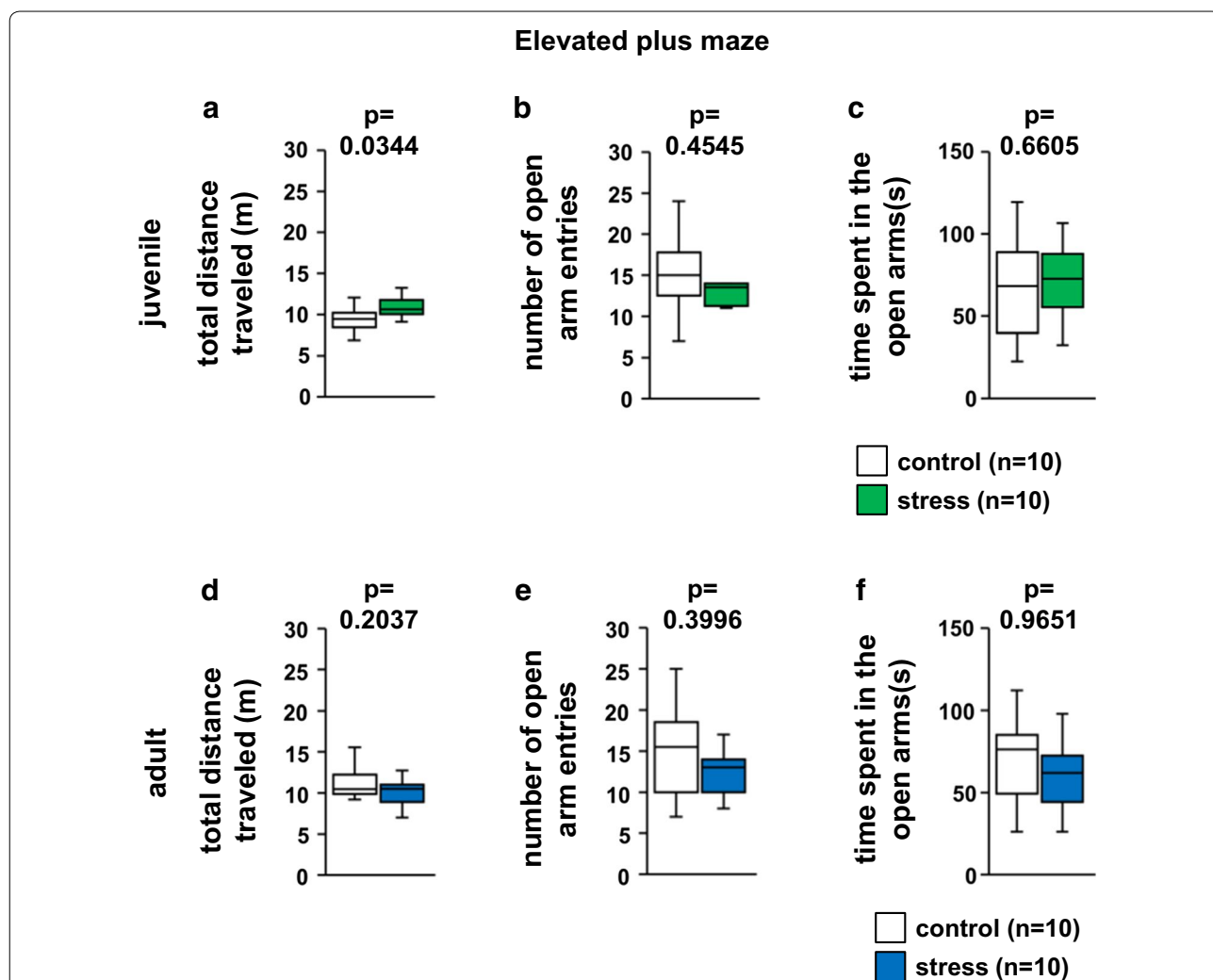
Fig. 3 Results of the elevated plus maze test in the stress and control groups. Juvenile: distance traveled (**a**), the number of open arm entries (**b**), and time spent in the open arms (**c**). Adult: distance traveled (**d**), the number of open arm entries (**e**), and time spent in the open arms (**f**). All data are presented as box plots. *Significant difference from control mice (p < 0.05). The p values were calculated by Student's t test (**a–f**)

Ueno *et al. BMC Neurosci* (2018) 19:41

Page 7 of 21
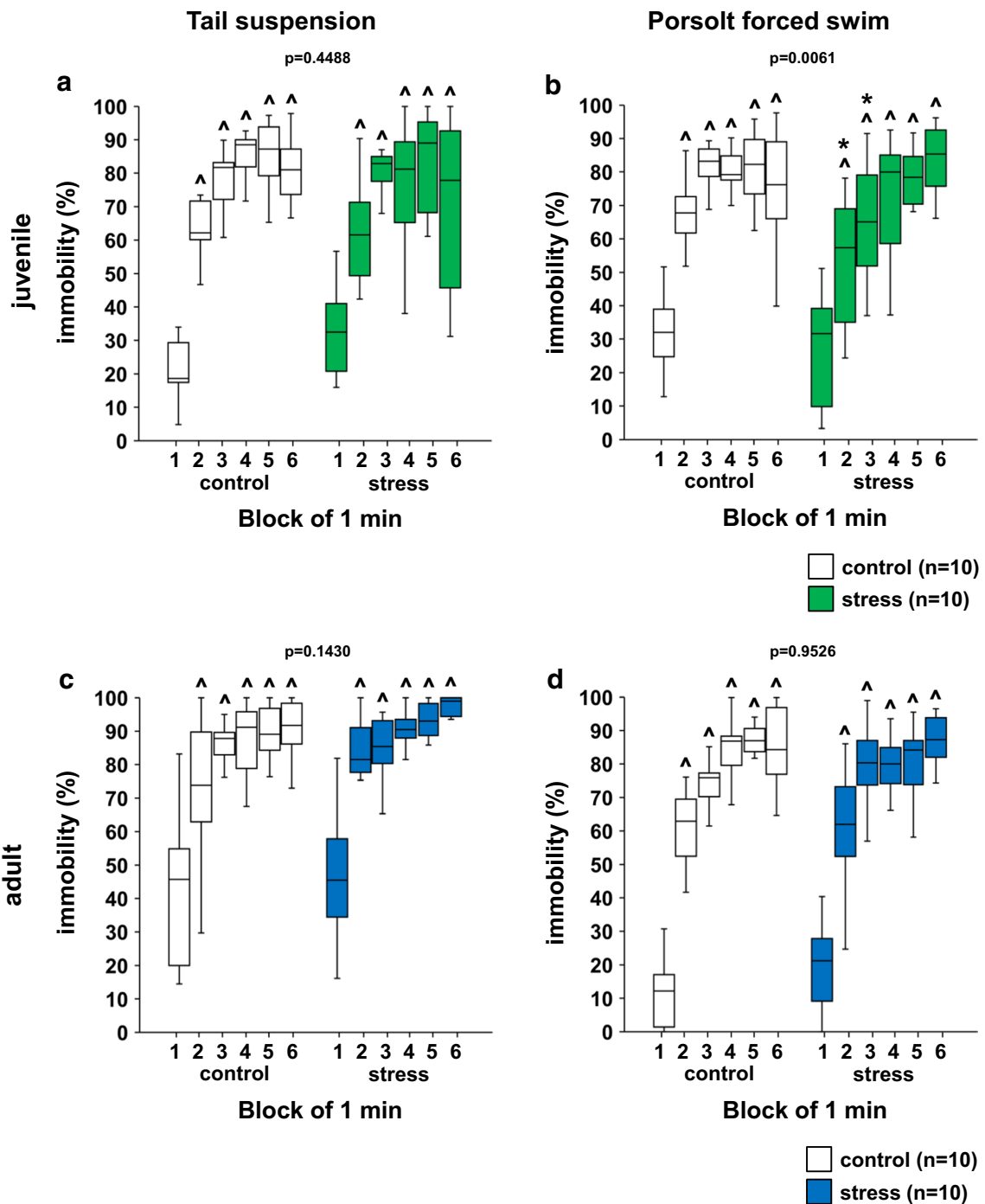
Fig. 4 Results of the tail-suspension test and Porsolt forced swim test in the stress and control groups. Juvenile: percentage of immobility time in each 1-min period (**a**) in the tail-suspension test. percentage of immobility time in each 1-min period (**b**) in the Porsolt forced swim test. Adult: percentage of immobility time in each 1-min period (**c**) in the tail-suspension test. Percentage of immobility time in each 1-min period (**d**) in the Porsolt forced swim test. All data are presented as box plots. *Significant difference from control mice ($p < 0.05$). ^$p < 0.05$ versus first block; *$p < 0.05$ between time-matched stress and control groups. The p values were calculated by two-way repeated measures ANOVA (**a**–**d**)

Ueno *et al. BMC Neurosci* (2018) 19:41

Page 8 of 21

Fig. 5 Results of the locomotor activity test in the stress and control groups. Juvenile: spontaneous locomotor activity in each 10-min period (**a**). Adult: spontaneous locomotor activity in each 10-min period (**b**). All data are presented as box plots. *Significant difference from control mice (p < 0.05). The p values were calculated by two-way repeated measures ANOVA (**a**, **b**)

the number of total entries, total distance traveled, and percentage of time spent in the open arms between the adult-stressed and control group mice (Fig. 3d, $t_{18} = 2.1098$, p = 0.2037; Fig. 3e, $t_{18} = 2.1098$, p = 0.3996; Fig. 3f, $t_{18} = 2.1098$, p = 0.9651).

Juvenile stress reduced depressive-like behaviors

We evaluated depressive-like behavior in juvenile stressed mice. In the tail-suspension test, there were no significant differences in the percentage of immobility time in each 1-min period during the 6-min test period between the juvenile-stressed and control group mice

(See figure on next page.)

Fig. 6 Results of the Social interaction test in the stress and control groups. Juvenile: time spent in the area (**a**), total distance traveled (**b**), number of entries around the cage (**c**), and time spent around the cage (**d**). Adult: time spent in the area (**e**), total distance traveled (**f**), number of entries around the cage (**g**), and time spent around the cage (**h**). All data are presented as box plots. *Significant difference from control mice (p < 0.05). The p values were calculated by two-way ANOVA (**a**, **c**, **d**, **e**, **g**, **h**), one-way ANOVA (**b**, **f**), and paired t test (between the same group in **a**, **c**, **d**, **e**, **g**, **h**)

Ueno *et al. BMC Neurosci* (2018) 19:41

Page 9 of 21

Social interaction test

Ueno *et al. BMC Neurosci* (2018) 19:41

Page 10 of 21

Fig. 7 Results of the Y-maze test in the stress and control groups. Juvenile: total distance traveled (**a**), total number of arm entries (**b**), total alternation (**c**), and percentage of alternation (**d**). Adult: total distance traveled (**e**), total number of arm entries (**f**), total alternation (**g**), and percentage of alternation (**h**). All data are presented as box plots. *Significant difference from control mice (p < 0.05). The p values were calculated by Student's t test (**a**–**h**)

(Fig. 4a, stress × time: $F_{1,102} = 0.578$, p = 0.4488; time in control: $F = 22.813$, p < 0.0001; time in stress group: $F = 13.792$, p < 0.0001). In the Porsolt forced swim test, the juvenile stressed mice spent significantly less time immobile in each 1-min period during the 6-min test period than did the control mice (Fig. 4b, stress × time: $F_{1,108} = 7.830$, p = 0.0061; time in control: $F = 16.349$, p < 0.0001; time in stress group: $F = 16.883$, p < 0.0001).
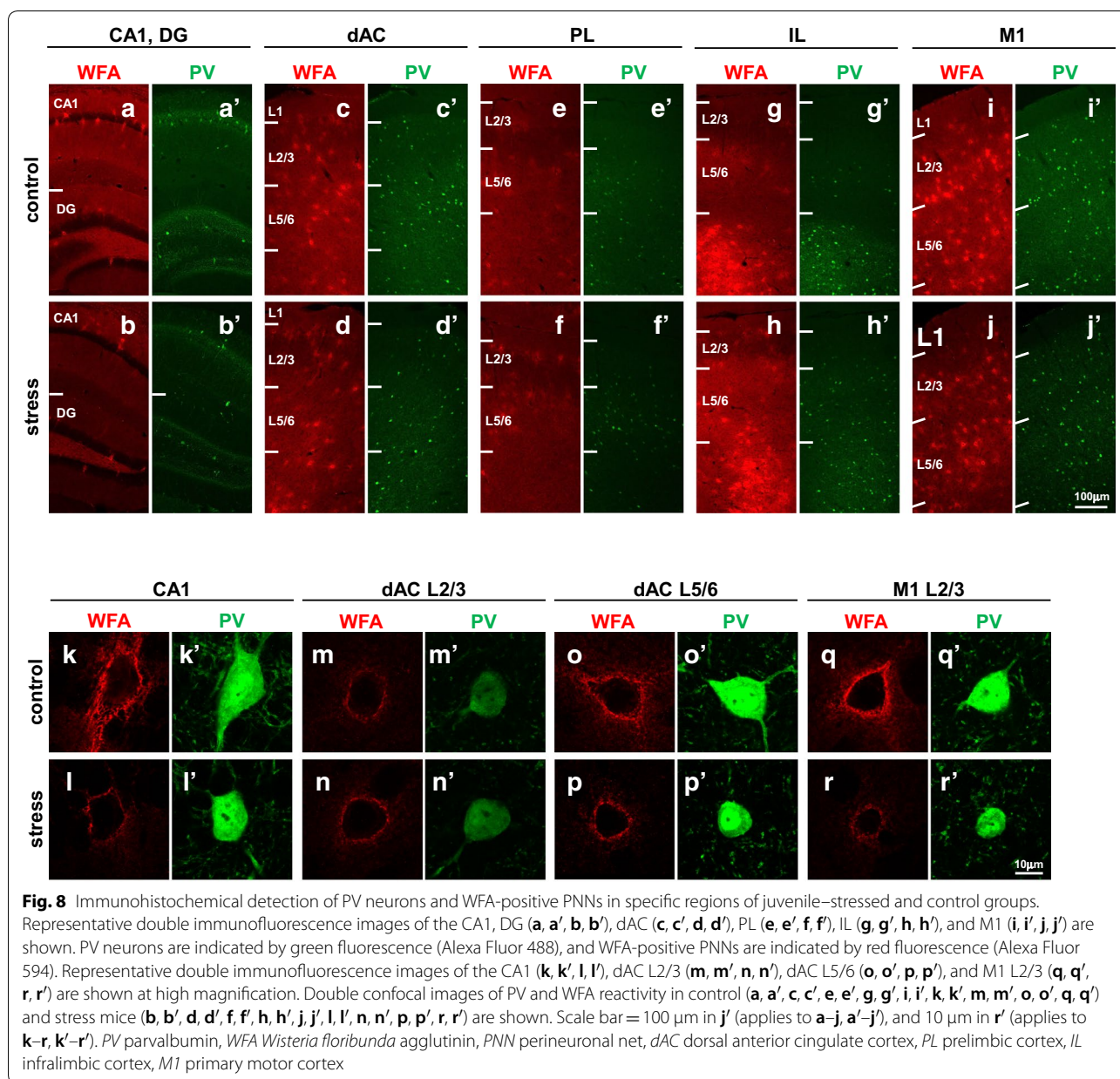
In the tail-suspension test, we found no significant differences between adult stressed and control mice (Fig. 4c, stress × time: $F_{1,108} = 2.176$, p = 0.1430; time in control: $F = 66.558$, p < 0.0001; time in stress group: $F = 50.135$, p < 0.0001). In the Porsolt forced swim test, during the 6-min test period, there were no significant differences in the percentage of immobility time in each 1-min period in the adult stressed than in the control mice (Fig. 4d, stress × time: $F_{1,108} = 0.004$, p = 0.9526; time in control: $F = 11.520$, p < 0.0001; time in stress group: $F = 12.582$, p < 0.0001).

Juvenile stress increased activity in a new environment

There were no significant differences in locomotor activity during the 150-min period between the adult juvenile stressed and control mice (Fig. 5a, $F_{1,210} = 1.200$, p = 0.2746; Fig. 5b, $F_{1,210} = 1.207$, p = 0.2732). For the first 30-min, we observed a significant increase in the locomotor activity in the juvenile-stressed compared with the control group mice (Fig. 5a, for the first 30-min; stress effect, $F_{1,42} = 12.750$, p = 0.0009; Fig. 5b, for the first 30-min; stress effect, $F_{1,42} = 1.476$, p = 0.2313).

Juvenile stress showed abnormal social behavior

In the social interaction test, we found several differences between juvenile stressed and control mice (Fig. 6a, $F_{1,36} = 3.434$, p = 0.072; Fig. 6c, $F_{1,36} = 20.774$, p < 0.0001; Fig. 6d, $F_{1,36} = 0.116$, p = 0.735). Control mice spent a significantly longer time in the area containing the novel (stranger) mouse in a transparent cage than in the area containing the empty cage (Fig. 6a, $t_9 = -2.147$, p = 0.060), but a similar amount of time in both around

Ueno *et al. BMC Neurosci (2018) 19:41*

Page 11 of 21

Fig. 8 Immunohistochemical detection of PV neurons and WFA-positive PNNs in specific regions of juvenile–stressed and control groups. Representative double immunofluorescence images of the CA1, DG (**a**, **a'**, **b**, **b'**), dAC (**c**, **c'**, **d**, **d'**), PL (**e**, **e'**, **f**, **f'**), IL (**g**, **g'**, **h**, **h'**), and M1 (**i**, **i'**, **j**, **j'**) are shown. PV neurons are indicated by green fluorescence (Alexa Fluor 488), and WFA-positive PNNs are indicated by red fluorescence (Alexa Fluor 594). Representative double immunofluorescence images of the CA1 (**k**, **k'**, **l**, **l'**), dAC L2/3 (**m**, **m'**, **n**, **n'**), dAC L5/6 (**o**, **o'**, **p**, **p'**), and M1 L2/3 (**q**, **q'**, **r**, **r'**) are shown at high magnification. Double confocal images of PV and WFA reactivity in control (**a**, **a'**, **c**, **c'**, **e**, **e'**, **g**, **g'**, **i**, **i'**, **k**, **k'**, **m**, **m'**, **o**, **o'**, **q**, **q'**) and stress mice (**b**, **b'**, **d**, **d'**, **f**, **f'**, **h**, **h'**, **j**, **j'**, **l**, **l'**, **n**, **n'**, **p**, **p'**, **r**, **r'**) are shown. Scale bar = 100 μm in **j'** (applies to **a–j**, **a'–j'**), and 10 μm in **r'** (applies to **k–r**, **k'–r'**). *PV* parvalbumin, *WFA Wisteria floribunda* agglutinin, *PNN* perineuronal net, *dAC* dorsal anterior cingulate cortex, *PL* prelimbic cortex, *IL* infralimbic cortex, *M1* primary motor cortex

cages (Fig. 6d, $t_9 = -1.695$, p = 0.124). Control mice increased the number of entries around the cage containing the stranger mouse than around empty cage (Fig. 6c, $t_9 = -4.839$, p = 0.001). In contrast, juvenile stressed mice spent a similar amount of time in both areas (Fig. 6a, $t_9 = -0.781$, p = 0.455), and had similar contact time with both cages (Fig. 6c, $t_9 = -3.783$, p = 0.004). During the 10-min period, juvenile stressed mice spent significantly more time around the cage containing the stranger mouse than around the empty cage (Fig. 6d, $t_9 = -1.638$, p = 0.136). There were no significant differences in the total distance traveled between juvenile stressed and control mice (Fig. 6b, $t_{18} = 2.1009$, p = 0.0797). Both control

and adult stressed mice spent a significantly longer time in the area containing the stranger mouse than in the area with the empty cage (Fig. 6e, $F_{1,36} = 0.0001$, p = 0.993, empty area versus stranger area: control, $t_9 = -3.408$, p = 0.008, stress, $t_9 = -3.950$, p = 0.003), and spent significantly more time around the cage containing the stranger mouse than around the empty cage (Fig. 6h, $F_{1,36} = 0.760$, p = 0.389, empty area versus stranger area: control, $t_9 = -3.244$, p = 0.010, stress, $t_9 = -2.281$, p = 0.048). Control mice had a similar number of contacts with both cages (Fig. 6g, $F_{1,36} = 1.010$, p = 0.322, empty area versus stranger area: control, $t_9 = -1.200$, p = 0.261). Adult stressed mice had an increased number of entries around

Ueno *et al. BMC Neurosci* (2018) 19:41

Page 12 of 21

the cage containing the stranger mouse than around the empty cage (Fig. 6g, $t_9 = -5.485$, p < 0.0001). During the 10-min period, there were no significant differences in the total distance traveled between adult stressed and control mice (Fig. 6f, $t_{18} = 2.1009$, p = 0.9639).

Juvenile stress did not change short-term spatial working memory

Short-term spatial working memory was examined by monitoring spontaneous alternation behavior in a Y-maze. There were no significant differences in these measures between the juvenile-stressed and control groups in the number of arm entries (Fig. 7b, $t_{18} = 2.1009$, p = 0.7144), in total alternations (Fig. 7c, $t_{18} = 2.1009$, p = 0.6303), alternation percentage (Fig. 7d, $t_{18} = 2.1009$, p = 0.4914), or total distance (Fig. 7a, $t_{18} = 2.1009$, p = 0.9832), indicating that juvenile stress did not affect short-term memory. The results for adult mice were similar (Fig. 7e, $t_{18} = 2.1009$, p = 0.0956; Fig. 7f, $t_{18} = 2.1009$, p = 0.2891; Fig. 7g, $t_{18} = 2.1009$, p = 0.3285; Fig. 7h, $t_{18} = 2.1009$, p = 0.8414).

Juvenile stress did not change the number of WFA-positive PNNs and PV neurons

We examined the effect of juvenile stress on the number of PV neurons and WFA-positive PNNs in several brain regions in juvenile stressed and control mice. Both PV neurons and WFA-positive PNNs were observed in all brain regions analyzed in this study (Fig. 8a–j, a′–j′).

In all brain regions analyzed in this study, there was no difference in the density of both PV neurons and WFA-positive PNNs between the juvenile stressed and control mice (Fig. 9a–f). There was no difference in the percentage of PV neurons enveloped by WFA-positive PNNs in

the hippocampus, prefrontal cortex, and primary motor cortex between the control and the juvenile stressed mice groups (Fig. 9g–i). In all brain regions analyzed in this study, the percentage of WFA-positive PNNs was similar between the juvenile stressed and control mice (Fig. 9j–l).

Juvenile stress reduces WFA-positive fluorescence intensity but does not change PV-positive fluorescence intensity

An enlarged image of PV neurons and WFA-positive PNNs under the same conditions is shown in Fig. 8, revealing that PV fluorescence intensity and WFA fluorescence intensity differed in each brain region (Fig. 8k–r, k′–r′). In addition, WFA fluorescence intensity differed between the control and juvenile stressed mice.

Analysis of fluorescence intensity revealed that both PV and WFA fluorescence intensities differed in each region and each cortical layer of the mouse brain (Fig. 10a–f). There were no differences in PV fluorescence intensity in the hippocampus, prefrontal cortex, and primary motor cortex between control and juvenile stressed mice (Fig. 10a–c). In the CA1 region of the hippocampus, WFA fluorescence intensity was lower in juvenile stressed than in control mice (Fig. 10d). In the dorsal anterior cingulate cortex (dAC) and infralimbic cortex (IL) parts of the prefrontal cortex in juvenile stressed mice, WFA fluorescence intensity was lower than in the same region in control mice (Fig. 10e). In the L2/3 of the primary motor cortex, WFA fluorescence intensity was lower in juvenile stressed than in control mice (Fig. 10f).

Juvenile stress reduces the soma of PV neurons

We also analyzed the soma of PV neurons in several brain regions of the juvenile stressed and control mice (Fig. 11). We analyzed 575 cells (dAC: L2/3 = 72; L5/6 = 72; PL:

(See figure on next page.)

Fig. 9 Densities of PV neurons and WFA-positive PNNs in juvenile-stressed or control mice. The region-specific patterns of PV neuron density (**a**–**c**) and WFA-positive PNN density (**d**–**f)** in individual regions are shown. The region-specific pattern of the percentage of PV neurons enveloped by WFA-positive PNNs (**g**–**i**) and the percentage of WFA-positive PNNs that contain PV (**j**–**l**) are shown in the individual regions, hippocampus (CA1, CA3, and DG) (**a**, **d**, **g**, **j**), prefrontal cortex (dAC, PL, and IL) (**b**, **e**, **h**, **k**), motor cortex (**c**, **f**, **i**, **l**) of control or stress mice. All data are presented as the mean ± SEM. *Significant difference from control mice (p < 0.05). The p values indicate two-way ANOVA by Bonferroni *t* test. Abbreviations are the same as those in Fig. 8. **a** Hippocampus; group: $F_{1,66} = 0.086$, region: $F_{2,66} = 6.449$, group × region: $F_{2,66} = 0.111$. CA1: p = 0.6254. CA3: p = 0.8485. DG: p = 0.8626, **b** prefrontal cortex; group: $F_{1,132} = 0.126$, region: $F_{5,132} = 48.755$, group × region: $F_{5,132} = 0.966$. dAC L2/3: p = 0.3783. dAC L5/6: p = 0.4354. PL L2/3: p = 0.9115. PL L5/6: p = 0.2392. IL L2/3: p = 0.9986. IL L5/6: p = 0.1444, **c** M1; group: $F_{1,44} = 1.140$, region: $F_{1,44} = 0.997$, group × region: $F_{1,44} = 0.002$. M1 L2/3: p = 0.4744. M1 L5/6: p = 0.4345, **d** hippocampus; group: $F_{1,66} = 0.134$, region: $F_{2,66} = 11.937$, group × region: $F_{2,66} = 0.618$. CA1: p = 0.09717. CA3: p = 0.2794. DG: p = 0.6745, **e** prefrontal cortex; group: $F_{1,132} = 0.895$, region: $F_{5,132} = 16.458$, group × region: $F_{5,132} = 0.476$. dAC L2/3: p = 0.4839. dAC L5/6: p = 0.3845. PL L2/3: p = 0.9320. PL L5/6: p = 0.3263. IL L2/3: p = 0.4270. IL L5/6: p = 0.5232, **f** M1; group: $F_{1,44} = 3.048$, region: $F_{1,44} = 0.636$, group × region: $F_{1,44} = 0.144$. M1 L2/3: p = 0.3391. M1 L5/6: p = 0.1401, **g** hippocampus; group: $F_{1,66} = 0.145$, region: $F_{2,66} = 1.550$, group × region: $F_{2,66} = 0.730$. CA1: p = 0.6958. CA3: p = 0.2359. DG: p = 0.8866, **h** prefrontal cortex; group: $F_{1,114} = 0.132$, region: $F_{5,114} = 9.911$, group × region: $F_{5,114} = 6.183$. dAC L2/3: p = 0.9590. dAC L5/6: p = 0.2913. PL L2/3: p = 0.3957. PL L5/6: p = 0.1294. IL L5/6: p = 0.4050, **i** M1; group: $F_{1,44} = 3.446$, region: $F_{1,44} = 0.060$, group × region: $F_{1,44} = 0.6514$. M1 L2/3: p = 0.1093. M1 L5/6: p = 0.3271, **j** hippocampus; group: $F_{1,66} = 0.012$, region: $F_{2,66} = 3.619$, group × region: $F_{2,66} = 0.617$. CA1: p = 0.4328. CA3: p = 0.8622. DG: p = 0.4441, **k** prefrontal cortex; group: $F_{1,116} = 0.886$, region: $F_{5,116} = 17.793$, group × region: $F_{5,116} = 0.905$. dAC L2/3: p = 0.9922. dAC L5/6: p = 0.2344. PL L2/3: p = 0.9398. PL L5/6: p = 0.1568. IL L2/3: p = 0.3948. IL L5/6: p = 0.2722, **l** M1; group: $F_{1,44} = 6.832$, region: $F_{1,44} = 3.364$, group × region: $F_{1,44} = 0.049$. M1 L2/3: p = 0.0977. M1 L5/6: p = 0.0512

Ueno *et al. BMC Neurosci* (2018) 19:41

Page 13 of 21
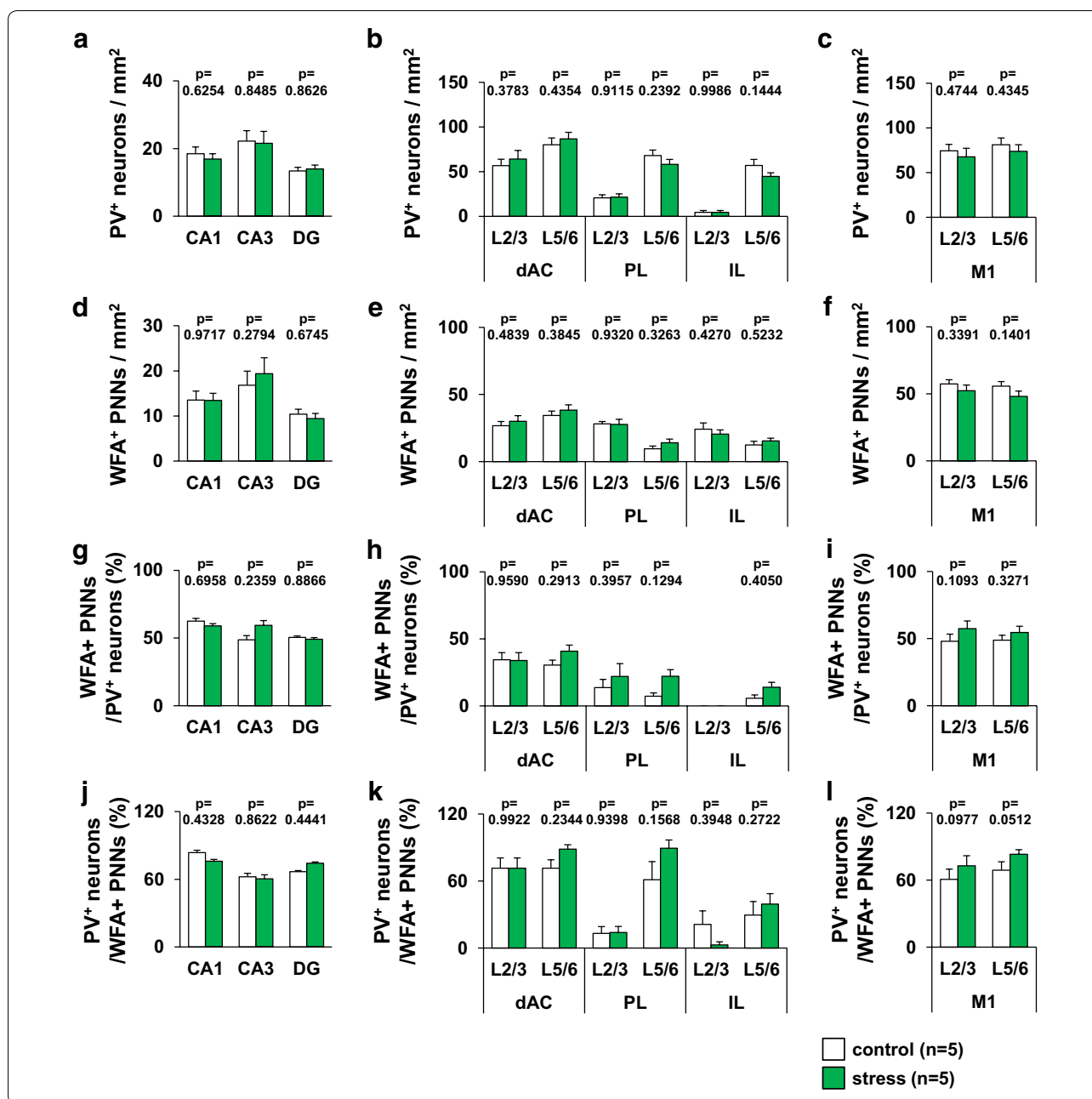
L2/3 = 40, L5/6 = 57; IL: L2/3 = 17, L5/6 = 65; M1: L2/3 = 71, L5/6 = 73; CA = 36; CA3 = 36; DG = 36) from control mice, and 567 cells (dAC: L2/3 = 66; L5/6 = 73; PL: L2/3 = 30, L5/6 = 65; IL: L2/3 = 14, L5/6 = 67; M1: L2/3 = 72, L5/6 = 72; CA = 36; CA3 = 36; DG = 36) from juvenile stressed mice. In the CA3 of the hippocampus and L2/3 of the dAC, the area of the soma of PV neurons was smaller in juvenile stressed than in control mice (Fig. 11a, b). No significant differences in soma size were found in the PV neurons of the primary motor

cortex between the control and the juvenile stressed mice groups (Fig. 11c).

Juvenile stress did not change the number of Cat-315-positive PNNs

We examined the effect of juvenile stress on the expression of aggrecan in several brain regions of the juvenile stressed and control mice. The anti-aggrecan antibody Cat-315 is frequently used as a marker of aggrecan-expression on PNNs. We observed more WFA-positive
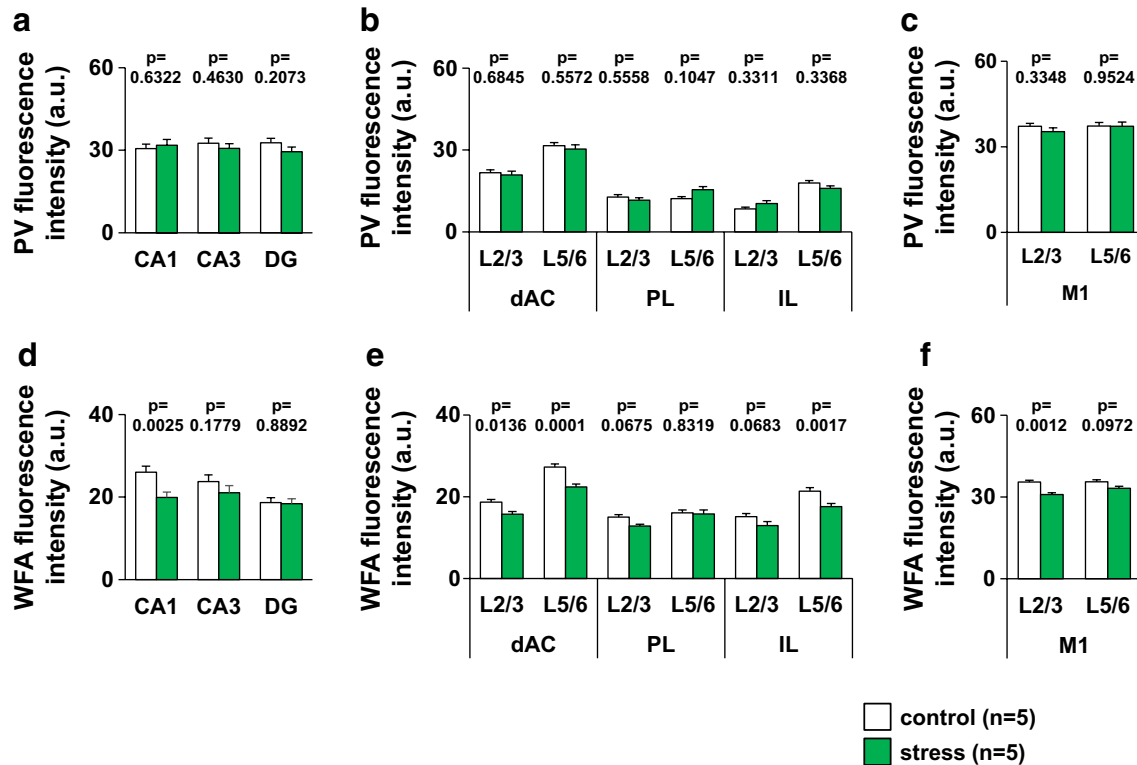
Ueno *et al. BMC Neurosci* (2018) 19:41

Page 14 of 21

Fig. 10 Fluorescence intensity of PV and WFA-positive PNN in each brain region of juvenile-stressed or control mice. Region-specific pattern of the mean fluorescence intensity of PV neurons (**a**–**c**) and WFA-positive PNNs (**d**–**f**) in the hippocampus (CA1, CA3, and DG), prefrontal cortex (dAC, PL, and IL), and motor cortex of control or stress mice. All data are presented as the mean ± SEM. *Significant difference from control mice (p < 0.05). The p values indicate two-way ANOVA by Bonferroni *t* test. Abbreviations are the same as those in Fig. 8. **a** hippocampus; group: $F_{1,210} = 0.771$, region: $F_{2,210} = 0.052$, group × region: $F_{2,210} = 0.800$. CA1: p = 0.6322. CA3: p = 0.4630. DG: p = 0.2073, **b** prefrontal cortex; group: $F_{1,626} = 0.001$, region: $F_{5,626} = 60.261$, group × region: $F_{5,626} = 1.073$. dAC L2/3: p = 0.6845. dAC L5/6: p = 0.5572. PL L2/3: p = 0.5558. PL L5/6: p = 0.1047. IL L2/3: p = 0.3311. IL L5/6: p = 0.3368, **c** M1; group: $F_{1,284} = 0.526$, region: $F_{1,284} = 0.474$, group × region: $F_{1,284} = 0.411$. M1 L2/3: p = 0.3348. M1 L5/6: p = 0.9524, **d** hippocampus; group: $F_{1,210} = 6.893$, region: $F_{2,210} = 5.811$, group × region: $F_{2,210} = 2.147$. CA1: p = 0.0025. CA3: p = 0.1779. DG: p = 0.8892, **e** prefrontal cortex; group: $F_{1,395} = 30.846$, region: $F_{5,395} = 48.052$, group × region: $F_{5,395} = 1.756$. dAC L2/3: p = 0.0136. dAC L5/6: p = 0.0001. PL L2/3: p = 0.0675. PL L5/6: p = 0.8319. IL L2/3: p = 0.0683. IL L5/6: p = 0.0017, **f** M1; group: $F_{1,320} = 12.119$, region: $F_{1,320} = 1.436$, group × region: $F_{1,320} = 1.274$. M1 L2/3: p = 0.0012. M1 L5/6: p = 0.0972

PNNs in the mouse cerebral cortex at P30, while in some brain regions, Cat-315-positive PNN was not yet expressed at P30 (Fig. 12a–d, a′–d′). We did not observe Cat-315-positive PNNs in the mouse prefrontal cortex.
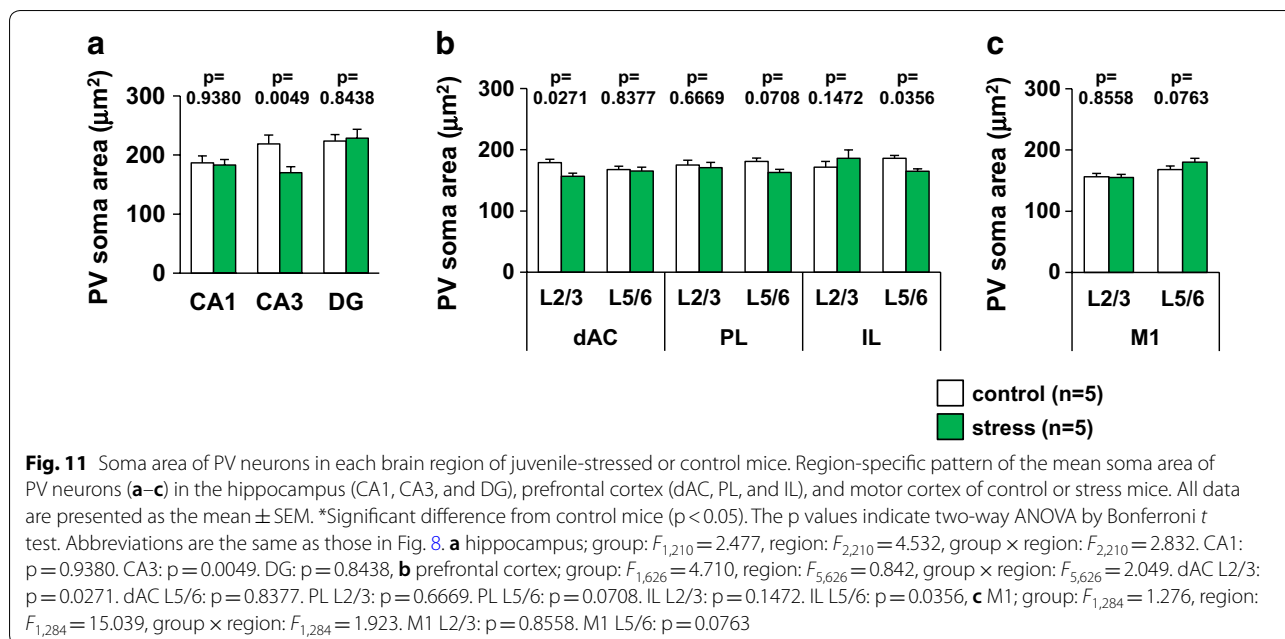
Further, we quantified the number of Cat-315-positive PNNs in the hippocampus and primary motor cortex of the juvenile stressed and control mice (Fig. 12e, f). There was no difference in the density of Cat-315-positive PNNs between juvenile stressed and control mice (Fig. 12e, f). To examine whether juvenile stress affects Cat-315-positive PNN component expression on WFA-positive PNNs in the hippocampus and primary motor cortex of juvenile stressed mice, we quantified the percentage of WFA-positive PNNs co-localized with Cat-315-positive PNNs, and it was similar between the juvenile stressed and control mice (Fig. 12g, h).

Juvenile stress did not affect immune activation in the central nervous system

To examine whether juvenile stress affects immune activation in the central nervous system of juvenile stressed mice, we observed the morphology of Iba-1-positive microglia in the hippocampus, prefrontal cortex, and primary motor cortex (Fig. 13). Monoclonal antibody Iba-1 is frequently used as a comprehensive marker of microglia. There was no significant difference in the morphology of Iba-1-positive microglia between the control and juvenile stressed mice in the hippocampus, prefrontal cortex, and primary motor cortex (Fig. 13).

Discussion

In this study, we investigated the influence of stress on behavioral abnormalities and on the development of PV neurons and WFA-positive PNNs in juvenile and adult

Ueno *et al. BMC Neurosci* (2018) 19:41

Page 15 of 21

Fig. 11 Soma area of PV neurons in each brain region of juvenile-stressed or control mice. Region-specific pattern of the mean soma area of PV neurons (**a**–**c**) in the hippocampus (CA1, CA3, and DG), prefrontal cortex (dAC, PL, and IL), and motor cortex of control or stress mice. All data are presented as the mean ± SEM. *Significant difference from control mice (p < 0.05). The p values indicate two-way ANOVA by Bonferroni *t* test. Abbreviations are the same as those in Fig. 8. **a** hippocampus; group: $F_{1,210} = 2.477$, region: $F_{2,210} = 4.532$, group × region: $F_{2,210} = 2.832$. CA1: p = 0.9380. CA3: p = 0.0049. DG: p = 0.8438, **b** prefrontal cortex; group: $F_{1,626} = 4.710$, region: $F_{5,626} = 0.842$, group × region: $F_{5,626} = 2.049$. dAC L2/3: p = 0.0271. dAC L5/6: p = 0.8377. PL L2/3: p = 0.6669. PL L5/6: p = 0.0708. IL L2/3: p = 0.1472. IL L5/6: p = 0.0356, **c** M1; group: $F_{1,284} = 1.276$, region: $F_{1,284} = 15.039$, group × region: $F_{1,284} = 1.923$. M1 L2/3: p = 0.8558. M1 L5/6: p = 0.0763
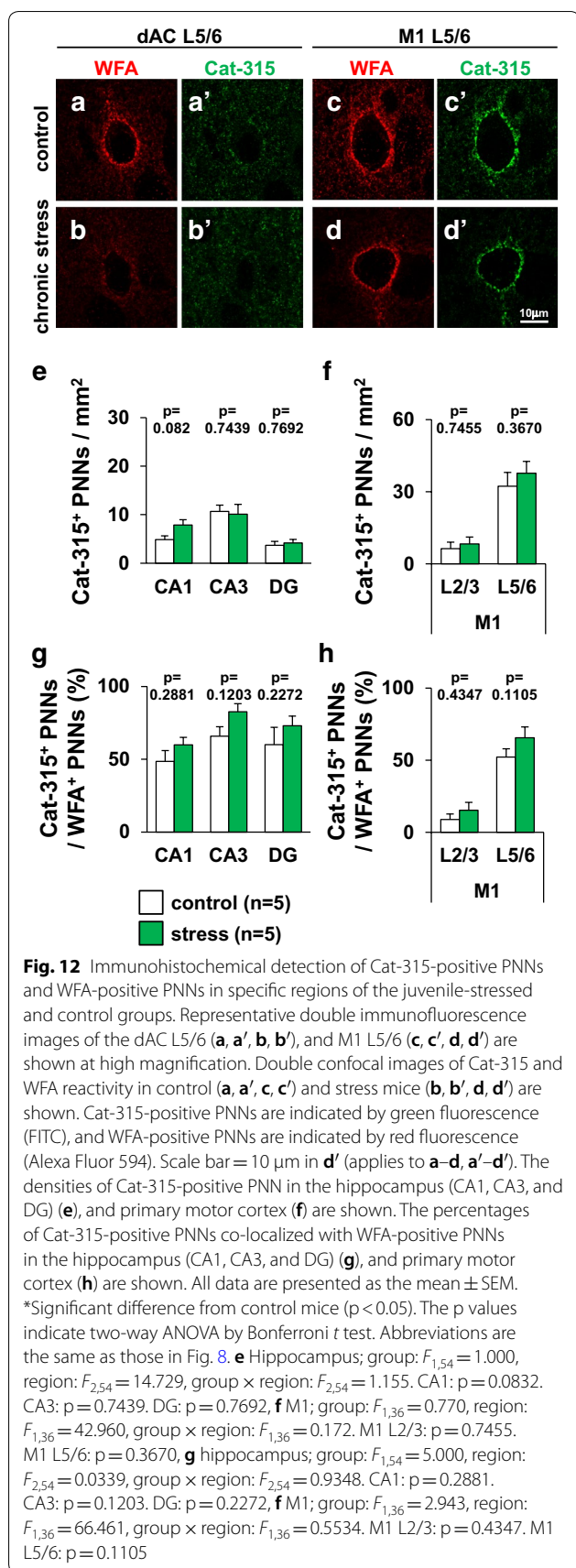
mice. We discovered that juvenile stress causes increased activity, decreased depressive-like behavior, and social deficits in mice. Furthermore, we revealed that the fluorescence intensity of WFA-positive PNNs decreased in the central nervous system of juvenile stressed mice. These results suggest that juvenile stress affects the development of the mouse brain and causes behavioral abnormalities different from those seen in the case of stressed mature mice.

Juvenile stressed mice had lower body weight and decreased grip strength than control mice. Using the present stress program, mature mice did not show physical changes. Previous studies using juvenile rats and mice also reported that body weight decreases owing to juvenile stress [70, 78]. Decreased essential enzyme secretion for normal cell growth, decreased DNA synthesis, and reduced growth hormone have been implicated as the underlying mechanisms [79, 80]. Indeed, in human studies, it has been reported that the weight of stressed adolescents is lower than that of healthy children [81]. Decreased body weight during the developmental stage may be an indication that the individual is experiencing stress [82].

In the new home cage, juvenile stressed mice showed excessive activity in the first 30 min compared to control mice. In the case of mature mice, such hyperactive behaviors were not observed. In mature mice, the activity level decreases or does not change owing to chronic stress [83–86]. Hyperactivity is a symptom of neuropsychiatric disorders, such as autism spectrum disorder (ASD), and attention deficit hyperactivity disorder (ADHD) [87–90].

Juvenile stressed mice had increased total distance traveled in the elevated plus maze test compared to control mice. An increased total distance seen in the elevated plus maze test may indicate increased locomotor activity or maladaptive-like behavior to the new environment [91]. However, in juvenile stressed mice, increased activity was not observed in all behavioral tests. There were no significant differences in the percentage of time spent in the open arms between the juvenile-stressed and control group mice in the elevated plus maze test. In studies using rats, decreased anxiety-like behavior caused by juvenile stress has been reported [92, 93]. Further studies are needed to elucidate the detailed mechanism.

In this study, depressive-like behavior was decreased in juvenile stressed mice in the Porsolt forced swim test, compared to control mice. Previous studies reported that depressive-like behaviors increase when the animals are exposed to chronic stress [94–98]. In this study, stressed mature mice did not show depressive-like behavior. This result may be due to a shorter stress period than that used in other chronically stressed models [78, 99]. Differences between juvenile stressed and adult stressed mice have also been reported in other studies [78]. It is suggested that these are due to differences in released corticosterone, hypothalamic–pituitary–adrenal depressive-like behavior function, and brain developmental stage [14, 100]. Further studies are needed to elucidate the detailed mechanism; however, based on our results, it is suggested that juvenile mice are more sensitive to stress than adult mice.
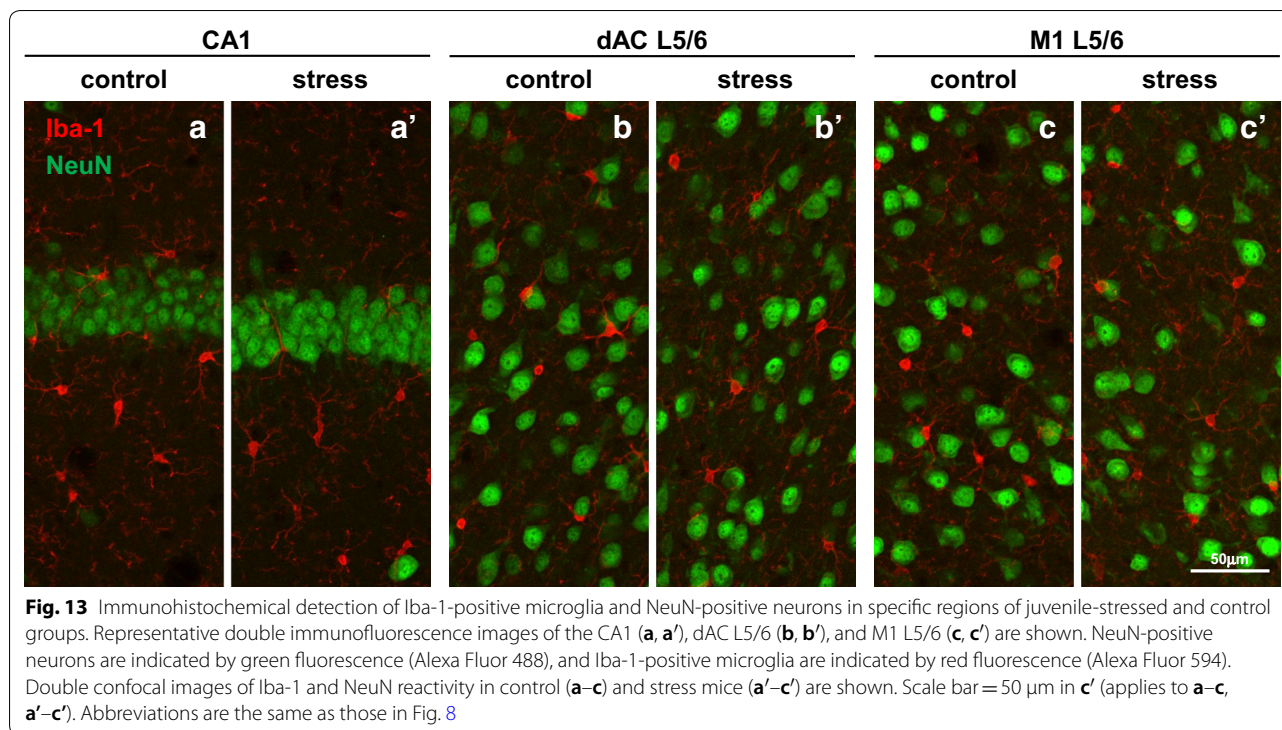
Ueno *et al. BMC Neurosci* (2018) 19:41

Page 16 of 21

Fig. 12 Immunohistochemical detection of Cat-315-positive PNNs and WFA-positive PNNs in specific regions of the juvenile-stressed and control groups. Representative double immunofluorescence images of the dAC L5/6 (**a**, **a′**, **b**, **b′**), and M1 L5/6 (**c**, **c′**, **d**, **d′**) are shown at high magnification. Double confocal images of Cat-315 and WFA reactivity in control (**a**, **a′**, **c**, **c′**) and stress mice (**b**, **b′**, **d**, **d′**) are shown. Cat-315-positive PNNs are indicated by green fluorescence (FITC), and WFA-positive PNNs are indicated by red fluorescence (Alexa Fluor 594). Scale bar = 10 μm in **d′** (applies to **a**–**d**, **a′**–**d′**). The densities of Cat-315-positive PNN in the hippocampus (CA1, CA3, and DG) (**e**), and primary motor cortex (**f**) are shown. The percentages of Cat-315-positive PNNs co-localized with WFA-positive PNNs in the hippocampus (CA1, CA3, and DG) (**g**), and primary motor cortex (**h**) are shown. All data are presented as the mean ± SEM. *Significant difference from control mice (p < 0.05). The p values indicate two-way ANOVA by Bonferroni *t* test. Abbreviations are the same as those in Fig. 8. **e** Hippocampus; group: $F_{1,54} = 1.000$, region: $F_{2,54} = 14.729$, group × region: $F_{2,54} = 1.155$. CA1: p = 0.0832. CA3: p = 0.7439. DG: p = 0.7692, **f** M1; group: $F_{1,36} = 0.770$, region: $F_{1,36} = 42.960$, group × region: $F_{1,36} = 0.172$. M1 L2/3: p = 0.7455. M1 L5/6: p = 0.3670, **g** hippocampus; group: $F_{1,54} = 5.000$, region: $F_{2,54} = 0.0339$, group × region: $F_{2,54} = 0.9348$. CA1: p = 0.2881. CA3: p = 0.1203. DG: p = 0.2272, **f** M1; group: $F_{1,36} = 2.943$, region: $F_{1,36} = 66.461$, group × region: $F_{1,36} = 0.5534$. M1 L2/3: p = 0.4347. M1 L5/6: p = 0.1105

In juvenile stressed mice, social preference to stranger mice was reduced compared with control mice. When adult mice were exposed to chronic stress, there was no reduction in sociability [101, 102]. When genetic abnormality occurs in the energy metabolism of PV neurons, social ability is altered in mice [103]. In mice deficient in PV protein, abnormal social behavior and decreased memory ability, such as those seen in ASD-like behavioral abnormalities was observed [46]. In this study, we found WFA-positive PNNs reduced fluorescence intensity around PV neurons in juvenile stressed mice, and it is possible that PV neurons were functioning abnormally. Therefore, in juvenile stressed mice, social preference to stranger mice was altered compared with control mice. Chronic stress affects social interaction and function of paraventricular nucleus [104, 105]. Even in juvenile stressed mice, there may be abnormality in paraventricular nucleus. Further research is necessary to elucidate this mechanism. Abnormal social behavior is a symptom of neuropsychiatric disorders, such as ASD, ADHD, and schizophrenia [106–108].

Adult mice showed an alternation percentage statistically above chance level (50% of alternation) whereas juvenile mice did not in a Y-maze. This indicates that this test is not reliable for juvenile mice.

Juvenile stressed mice showed decreased depressive-like behavior, increased locomotor activity, and abnormal social behavior compared to control mice. It was revealed that chronically stressed juvenile mice showed ADHD- and ASD-like behavioral abnormalities. As described below, there is a possibility that this behavior was caused by PV neuron dysfunction due to decreased PNN condense.

In recent years, it has been shown that the balance between excitation and inhibition in the central nervous system is important for normal brain activity, and any imbalance is believed to cause neuropsychiatric disorder-like behaviors [109, 110]. Abnormalities in the PV neurons have been shown postmortem in the brains of patients with neuropsychiatric disorders, such as schizophrenia and depression [26, 111]. In experimental models, pups born to dams stressed during pregnancy show behavioral abnormalities, indicating decrease in the number of cortical PV neurons and WFA-positive PNNs [112]. The development of PV neurons in the sensory cortex is dependent on sensory inputs, and the development of PV neurons is delayed when sensory inputs are deprived [113–116]. In this study, stress was applied to juvenile mice, but there was no change in both the number of PV neurons and the number of WFA-positive PNNs in the hippocampus, prefrontal cortex, and primary motor cortex. It has been reported that *Vicia villosa* agglutinin (VVA)-positive PNNs increase in the

Ueno *et al. BMC Neurosci (2018) 19:41*

Page 17 of 21

Fig. 13 Immunohistochemical detection of Iba-1-positive microglia and NeuN-positive neurons in specific regions of juvenile-stressed and control groups. Representative double immunofluorescence images of the CA1 (**a**, **a'**), dAC L5/6 (**b**, **b'**), and M1 L5/6 (**c**, **c'**) are shown. NeuN-positive neurons are indicated by green fluorescence (Alexa Fluor 488), and Iba-1-positive microglia are indicated by red fluorescence (Alexa Fluor 594). Double confocal images of Iba-1 and NeuN reactivity in control (**a**–**c**) and stress mice (**a'**–**c'**) are shown. Scale bar = 50 μm in **c'** (applies to **a**–**c**, **a'**–**c'**). Abbreviations are the same as those in Fig. 8

prefrontal cortex of juvenilehood stressed rats within a few weeks [93]. This study showed that stress applied to juvenile mice for approximately 1 week had no obvious influence on the development of PV neurons.

In this study, it was revealed that the fluorescence intensity of WFA-positive PNN in juvenile stressed mice was decreased in the hippocampus, prefrontal cortex, and primary motor cortex compared to control mice. The PNN is a structure enriched with a special extracellular matrix molecule, and a decreased fluorescence intensity is presumed to signify decreased concentration or change in PNN components [115, 116]. Therefore, it is suggested that there was increased synaptic plasticity and increased vulnerability in the brains of juvenile stressed mice compared with control mice. When genetic abnormality occurs in the PNNs formation, social ability is altered in mice [117–119]. It has been reported that stress at a young age changes the hippocampus structurally and functionally [120, 121]. Juvenile stress causes structural and functional changes in the hippocampus [120, 121]. Both the hippocampus and prefrontal cortex are areas vulnerable to stress [62, 122, 123]. In particular, these areas are sensitive to stress during early childhood and adolescence [124, 125]. It has been reported that experiences in early life dramatically alter the structure and function of the brain after maturation [13, 122], and the alterations in PNN extracellular matrix molecules observed in this study could be maintained until maturity [91]. Epidemiological studies have shown that juvenile stress is associated with depression, anxiety, PTSD, and suicide development in adulthood [126, 127]. Chronic stress activates microglia in the central nervous system [128]. However, in this study we have not confirm the activated microglia image. Further studies are needed to elucidate the mechanism of PNN abnormality obtained in this study.

Conclusions

The present results indicate that juvenile stress affects brain development and causes behavioral abnormalities resembling behaviors linked to developmental disorders in mice. Juvenile individuals are more sensitive and respond differently to stress than mature individuals. The study results may help establish a method to prevent the onset of neuropsychiatric disorders in both juvenilehood and adolescence.

Ueno *et al. BMC Neurosci* (2018) 19:41

Page 18 of 21

Study concept and design. HU, SS: Acquisition of data. HU, SS: Analysis and interpretation of data. HU, MO: Drafting of the manuscript. SM, NK, KW, YM, SA, TI: Critical revision of the manuscript for important intellectual content. HU, SS: Statistical analysis. MO, SA, TI: Study supervision. All authors read and approved the final manuscript.

Author details
[1] Department of Medical Technology, Kawasaki University of Medical Welfare, 288, Matsushima, Kurashiki, Okayama 701-0193, Japan. [2] Department of Medical Technology, Graduate School of Health Sciences, Okayama University, Okayama 700-8558, Japan. [3] Department of Psychiatry, Kawasaki Medical School, Kurashiki 701-0192, Japan. [4] Department of Neuropsychiatry, Graduate School of Medicine, Dentistry and Pharmaceutical Sciences, Okayama University, Okayama 700-8558, Japan.

Competing interests
The authors declare that they have no competing interests.

Availability of data and materials
The datasets used and/or analysed during the current study are available from the corresponding author on reasonable request.

Consent for publication
Not applicable.

Ethics approval and consent to participate
All animal experiments were performed in accordance with the U.S. National Institutes of Health (NIH)—Guide for the Care and Use of Laboratory Animals (NIH Publication No. 80-23, revised in 1996) and approved by the Committee for Animal Experiments at the Kawasaki Medical School Advanced Research Center (Animal Project No. 17-084).

Publisher's Note
Springer Nature remains neutral with regard to jurisdictional claims in published maps and institutional affiliations.

References
1. Costello EJ, Mustillo S, Erkanli A, Keeler G, Angold A. Prevalence and development of psychiatric disorders in childhood and adolescence. Arch Gen Psychiatry. 2003;60:837–44.
2. Jones PB. Adult mental health disorders and their age at onset. Br J Psychiatry Suppl. 2013;54:5–10.
3. Kessler RC, Berglund P, Demler O, Jin R, Merikangas KR, Walters EE. Lifetime prevalence and age-of-onset distributions of DSM-IV disorders in the National Comorbidity Survey Replication. Arch Gen Psychiatry. 2005;62:593–602.
4. Turner RJ, Lloyd DA. Stress burden and the lifetime incidence of psychiatric disorder in young adults: racial and ethnic contrasts. Arch Gen Psychiatry. 2004;61:481–8.
5. Pelcovitz D, Kaplan S, Goldenberg B, Mandel F, Lehane J, Guarrera J. Post-traumatic stress disorder in physically abused adolescents. J Am Acad Child Adolesc Psychiatry. 1994;33:305–12.
6. Finkelhor D, Cross TP, Cantor EN. The justice system for juvenile victims: a comprehensive model of case flow. Trauma Violence Abuse. 2005;6:83–102.
7. Dunn VJ, Abbott RA, Croudace TJ, Wilkinson P, Jones PB, Herbert J, Goodyer IM. Profiles of family-focused adverse experiences through childhood and early adolescence: the ROOTS project a community investigation of adolescent mental health. BMC Psychiatry. 2011;11:109.
8. Shanahan L, Copeland WE, Costello EJ, Angold A. Child-, adolescent- and young adult-onset depressions: differential risk factors in development? Psychol Med. 2011;41:2265–74.
9. Kendler KS, Karkowski LM, Prescott CA. Causal relationship between stressful life events and the onset of major depression. Am J Psychiatry. 1999;156:837–41.
10. Blakemore SJ. Development of the social brain during adolescence. Q J Exp Psychol (Hove). 2008;61:40–9.
11. Caspi A, Roberts BW, Shiner RL. Personality development: stability and change. Annu Rev Psychol. 2005;56:453–84.
12. Gunnar M, Quevedo K. The neurobiology of stress and development. Annu Rev Psychol. 2007;58:145–73.
13. Romeo RD, McEwen BS. Stress and the adolescent brain. Ann N Y Acad Sci. 1094;2006:202–14.
14. Spear LP. The adolescent brain and age-related behavioral manifestations. Neurosci Biobehav Rev. 2000;24:417–63.
15. Casey BJ, Jones RM. Neurobiology of the adolescent brain and behavior: implications for substance use disorders. J Am Acad Child Adolesc Psychiatry. 2010;49:1189–201.
16. Avital A, Richter-Levin G. Exposure to juvenile stress exacerbates the behavioural consequences of exposure to stress in the adult rat. Int J Neuropsychopharmacol. 2005;8:163–73.
17. Pohl J, Olmstead MC, Wynne-Edwards KE, Harkness K, Menard JL. Repeated exposure to stress across the childhood-adolescent period alters rats' anxiety- and depression-like behaviors in adulthood: the importance of stressor type and gender. Behav Neurosci. 2007;121:462–74.
18. Isgor C, Kabbaj M, Akil H, Watson SJ. Delayed effects of chronic variable stress during peripubertal-juvenile period on hippocampal morphology and on cognitive and stress axis functions in rats. Hippocampus. 2004;14:636–48.
19. Barha CK, Brummelte S, Lieblich SE, Galea LA. Chronic restraint stress in adolescence differentially influences hypothalamic–pituitary–adrenal axis function and adult hippocampal neurogenesis in male and female rats. Hippocampus. 2011;21:1216–27.
20. McEwen BS. The neurobiology of stress: from serendipity to clinical relevance. Brain Res. 2000;886:172–89.
21. Agoglia AE, Holstein SE, Small AT, Spanos M, Burrus BM, Hodge CW. Comparison of the adolescent and adult mouse prefrontal cortex proteome. PLoS ONE. 2017;12:e0178391.
22. Semple BD, Blomgren K, Gimlin K, Ferriero DM, Noble-Haeusslein LJ. Brain development in rodents and humans: identifying benchmarks of maturation and vulnerability to injury across species. Prog Neurobiol. 2013;106–107:1–16.
23. Bernheim A, Halfon O, Boutrel B. Controversies about the enhanced vulnerability of the adolescent brain to develop addiction. Front Pharmacol. 2013;4:118.
24. Rice F, Harold GT, Thapar A. Negative life events as an account of age-related differences in the genetic aetiology of depression in childhood and adolescence. J Child Psychol Psychiatry. 2003;44:977–87.
25. Romeo RD. Adolescence: a central event in shaping stress reactivity. Dev Psychobiol. 2010;52:244–53.
26. Lewis DA, Curley AA, Glausier JR, Volk DW. Cortical parvalbumin interneurons and cognitive dysfunction in schizophrenia. Trends Neurosci. 2012;35:57–67.
27. Beasley CL, Reynolds GP. Parvalbumin-immunoreactive neurons are reduced in the prefrontal cortex of schizophrenics. Schizophr Res. 1997;24:349–55.
28. Khundakar A, Morris C, Thomas AJ. The immunohistochemical examination of GABAergic interneuron markers in the dorsolateral prefrontal cortex of patients with late-life depression. Int Psychogeriatr. 2011;23:644–53.
29. Sauer JF, Strüber M, Bartos M. Impaired fast-spiking interneuron function in a genetic mouse model of depression. Elife. 2015;4:e04979.
30. Liang D, Li G, Liao X, Yu D, Wu J, Zhang M. Developmental loss of parvalbumin-positive cells in the prefrontal cortex and psychiatric

Ueno *et al. BMC Neurosci* (2018) 19:41

Page 19 of 21

anxiety after intermittent hypoxia exposures in neonatal rats might be mediated by NADPH oxidase-2. Behav Brain Res. 2016;296:134–40.

31. Tovote P, Fadok JP, Lüthi A. Neuronal circuits for fear and anxiety. Nat Rev Neurosci. 2015;16:317–31.

32. Zou D, Chen L, Deng D, Jiang D, Dong F, McSweeney C, Zhou Y, Liu L, Chen G, Wu Y, Mao Y. DREADD in parvalbumin interneurons of the dentate gyrus modulates anxiety, social interaction and memory extinction. Curr Mol Med. 2016;16:91–102.

33. Butt SJ, Stacey JA, Teramoto Y, Vagnoni C. A role for GABAergic interneuron diversity in circuit development and plasticity of the neonatal cerebral cortex. Curr Opin Neurobiol. 2017;43:149–55.

34. Sultan KT, Shi SH. Generation of diverse cortical inhibitory interneurons. Wiley Interdiscip Rev Dev Biol. 2018. https://doi.org/10.1002/wdev.306.

35. Wood KC, Blackwell JM, Geffen MN. Cortical inhibitory interneurons control sensory processing. Curr Opin Neurobiol. 2017;46:200–7.

36. Chu J, Anderson SA. Development of cortical interneurons. Neuropsychopharmacology. 2015;40:16–23.

37. Gonzalez-Burgos G, Cho RY, Lewis DA. Alterations in cortical network oscillations and parvalbumin neurons in schizophrenia. Biol Psychiatry. 2015;77:1031–40.

38. Takano T. Interneuron dysfunction in syndromic autism: recent advances. Dev Neurosci. 2015;37:467–75.

39. Jacob J. Cortical interneuron dysfunction in epilepsy associated with autism spectrum disorders. Epilepsia. 2016;57:182–93.

40. Konradi C, Yang CK, Zimmerman EI, Lohmann KM, Gresch P, Pantazopoulos H, Berretta S, Heckers S. Hippocampal interneurons are abnormal in schizophrenia. Schizophr Res. 2011;131:165–73.

41. Urakawa S, Takamoto K, Hori E, Sakai N, Ono T, Nishijo H. Rearing in enriched environment increases parvalbumin-positive small neurons in the amygdala and decreases anxiety-like behavior of male rats. BMC Neurosci. 2013;14:13.

42. Le Magueresse C, Monyer H. GABAergic interneurons shape the functional maturation of the cortex. Neuron. 2013;77:388–405.

43. Patz S, Grabert J, Gorba T, Wirth MJ, Wahle P. Parvalbumin expression in visual cortical interneurons depends on neuronal activity and TrkB ligands during an Early period of postnatal development. Cereb Cortex. 2004;14:342–51.

44. Sohal VS, Zhang F, Yizhar O, Deisseroth K. Parvalbumin neurons and gamma rhythms enhance cortical circuit performance. Nature. 2009;459:698–702.

45. Massi L, Lagler M, Hartwich K, Borhegyi Z, Somogyi P, Klausberger T. Temporal dynamics of parvalbumin-expressing axo-axonic and basket cells in the rat medial prefrontal cortex in vivo. J Neurosci. 2012;32:16496–502.

46. Wöhr M, Orduz D, Gregory P, Moreno H, Khan U, Vörckel KJ, Wolfer DP, Welzl H, Gall D, Schiffmann SN, Schwaller B. Lack of parvalbumin in mice leads to behavioral deficits relevant to all human autism core symptoms and related neural morphofunctional abnormalities. Transl Psychiatry. 2015;5:e525.

47. Xenos D, Kamceva M, Tomasi S, Cardin JA, Schwartz ML, Vaccarino FM. Loss of TrkB signaling in parvalbumin-expressing basket cells results in network activity disruption and abnormal behavior. Cereb Cortex. 2017;18:1–15.

48. Song I, Dityatev A. Crosstalk between glia, extracellular matrix and neurons. Brain Res Bull. 2018;136:101–8.

49. Slaker M, Blacktop JM, Sorg BA. Caught in the net: perineuronal nets and addiction. Neural Plast. 2016;2016:7538208.

50. Giamanco KA, Matthews RT. Deconstructing the perineuronal net: cellular contributions and molecular composition of the neuronal extracellular matrix. Neuroscience. 2012;218:367–84.

51. Kwok JC, Carulli D, Fawcett JW. In vitro modeling of perineuronal nets: hyaluronan synthase and link protein are necessary for their formation and integrity. J Neurochem. 2010;114:1447–59.

52. Bandtlow CE, Zimmermann DR. Proteoglycans in the developing brain: new conceptual insights for old proteins. Physiol Rev. 2000;80:1267–90.

53. Yamaguchi Y. Lecticans: organizers of the brain extracellular matrix. Cell Mol Life Sci. 2000;57:276–89.

54. Seeger G, Lüth HJ, Winkelmann E, Brauer K. Distribution patterns of *Wisteria floribunda* agglutinin binding sites and parvalbumin-immunoreactive neurons in the human visual cortex: a double-labelling study. J Hirnforsch. 1996;37:351–66.

55. Slaker M, Blacktop JM, Sorg BA. Caught in the net: perineuronal nets and addiction. Neural Plast. 2016;2016:7538208.

56. Hensch TK. Critical period plasticity in local cortical circuits. Nat Rev Neurosci. 2005;6:877–88.

57. Lensjø KK, Lepperød ME, Dick G, Hafting T, Fyhn M. Removal of perineuronal nets unlocks juvenile plasticity through network mechanisms of decreased inhibition and increased gamma activity. J Neurosci. 2017;37:1269–83.

58. Pizzorusso T, Medini P, Berardi N, Chierzi S, Fawcett JW, Maffei L. Reactivation of ocular dominance plasticity in the adult visual cortex. Science. 2002;298:1248–51.

59. Balmer TS. Perineuronal nets enhance the excitability of fast-spiking neurons. eNeuro. 2016;3:4.

60. Fawcett JW. The extracellular matrix in plasticity and regeneration after CNS injury and neurodegenerative disease. Prog Brain Res. 2015;218:213–26.

61. Cabungcal JH, Steullet P, Morishita H, Kraftsik R, Cuenod M, Hensch TK, Do KQ. Perineuronal nets protect fast-spiking neurons against oxidative stress. Proc Natl Acad Sci USA. 2013;110:9130–5.

62. Ueno H, Suemitsu S, Murakami S, Kitamura N, Wani K, Okamoto M, Matsumoto Y, Ishihara T. Region-specific impairments in parvalbumin interneurons in social isolation-reared mice. Neuroscience. 2017;359:196–208.

63. De Luca C, Papa M. Looking inside the matrix: perineuronal nets in plasticity, maladaptive plasticity and neurological disorders. Neurochem Res. 2016;41:1507–15.

64. Pantazopoulos H, Berretta S. In sickness and in health: perineuronal nets and synaptic plasticity in psychiatric disorders. Neural Plast. 2016;2016:9847696.

65. Yoshioka N, Miyata S, Tamada A, Watanabe Y, Kawasaki A, Kitagawa H, Takao K, Miyakawa T, Takeuchi K, Igarashi M. Abnormalities in perineuronal nets and behavior in mice lacking CSGalNAcT1, a key enzyme in chondroitin sulfate synthesis. Mol Brain. 2017;10:47.

66. Banerjee SB, Gutzeit VA, Baman J, Aoued HS, Doshi NK, Liu RC, Ressler KJ. Perineuronal nets in the adult sensory cortex are necessary for fear learning. Neuron. 2017;95:169–79.

67. Popelář J, Díaz Gómez M, Lindovský J, Rybalko N, Burianová J, Oohashi T, Syka J. The absence of brain-specific link protein Bral2 in perineuronal nets hampers auditory temporal resolution and neural adaptation in mice. Physiol Res. 2017;66:867–80.

68. Umemori J, Takao K, Koshimizu H, Hattori S, Furuse T, Wakana S, Miyakawa T. ENU-mutagenesis mice with a non-synonymous mutation in Grin1 exhibit abnormal anxiety-like behaviors, impaired fear memory, and decreased acoustic startle response. BMC Res Notes. 2013;6:203.

69. Watanabe Y, Tsujimura A, Takao K, Nishi K, Ito Y, Yasuhara Y, Nakatomi Y, Yokoyama C, Fukui K, Miyakawa T, Tanaka M. Relaxin-3-deficient mice showed slight alteration in anxiety-related behavior. Front Behav Neurosci. 2011;5:50.

70. Brydges NM, Hall L, Nicolson R, Holmes MC, Hall J. The effects of juvenile stress on anxiety, cognitive bias and decision making in adulthood: a rat model. PLoS ONE. 2012;7:e48143.

71. Ducottet C, Griebel G, Belzung C. Effects of the selective nonpeptide corticotropin-releasing factor receptor 1 antagonist antalarmin in the chronic mild stress model of depression in mice. Prog Neuropsychopharmacol Biol Psychiatry. 2003;27:625–31.

72. Willner P, Towell A, Sampson D, Sophokleous S, Muscat R. Reduction of sucrose preference by chronic unpredictable mild stress, and its restoration by a tricyclic antidepressant. Psychopharmacology. 1987;93:358–64.

73. Li YF, Chen HX, Liu Y, Zhang YZ, Liu YQ, Li J. Agmatine increases proliferation of cultured hippocampal progenitor cells and hippocampal neurogenesis in chronically stressed mice. Acta Pharmacol Sin. 2006;27:1395–400.

74. Nakatani J, Tamada K, Hatanaka F, Ise S, Ohta H, Inoue K, Tomonaga S, Watanabe Y, Chung YJ, Banerjee R, Iwamoto K, Kato T, Okazawa M, Yamauchi K, Tanda K, Takao K, Miyakawa T, Bradley A, Takumi T. Abnormal behavior in a chromosome-engineered mouse model for human 15q11-13 duplication seen in autism. Cell. 2009;137:1235–46.

75. Tamada K, Tomonaga S, Hatanaka F, Nakai N, Takao K, Miyakawa T, Nakatani J, Takumi T. Decreased exploratory activity in a mouse model

Ueno *et al. BMC Neurosci* (2018) 19:41

Page 20 of 21

of 15q duplication syndrome; implications for disturbance of serotonin signaling. PLoS ONE. 2010;15:e15126.

76. Kouzu Y, Moriya T, Takeshima H, Yoshioka T, Shibata S. Mutant mice lacking ryanodine receptor type 3 exhibit deficits of contextual fear conditioning and activation of calcium/calmodulin-dependent protein kinase II in the hippocampus. Brain Res Mol Brain Res. 2000;76:142–50.

77. Ueno H, Suemitsu S, Matsumoto Y, Okamoto M. Sensory deprivation during early postnatal period alters the density of interneurons in the mouse prefrontal cortex. Neural Plast. 2015;2015:753179.

78. Sadler AM, Bailey SJ. Repeated daily restraint stress induces adaptive behavioural changes in both adult and juvenile mice. Physiol Behav. 2016;167:313–23.

79. Chapillon P, Patin V, Roy V, Vincent A, Caston J. Effects of pre- and post-natal stimulation on developmental, emotional, and cognitive aspects in rodents: a review. Dev Psychobiol. 2002;41:373–87.

80. Viveros MP, Llorente R, Díaz F, Romero-Zerbo SY, Bermudez-Silva FJ, Rodríguez de Fonseca F, Argente J, Chowen JA. Maternal deprivation has sexually dimorphic long-term effects on hypothalamic cell-turnover, body weight and circulating hormone levels. Horm Behav. 2010;58:808–19.

81. van Jaarsveld CH, Fidler JA, Steptoe A, Boniface D, Wardle J. Perceived stress and weight gain in adolescence: a longitudinal analysis. Obesity (Silver Spring). 2009;17:2155–61.

82. Jeong JY, Lee DH, Kang SS. Effects of chronic restraint stress on body weight, food intake, and hypothalamic gene expressions in mice. Endocrinol Metab. 2013;28:288–96.

83. Litteljohn D, Nelson E, Hayley S. IFN-γ differentially modulates memory-related processes under basal and chronic stressor conditions. Front Cell Neurosci. 2014;8:391.

84. DeVallance E, Riggs D, Jackson B, Parkulo T, Zaslau S, Chantler PD, Olfert IM, Bryner RW. Effect of chronic stress on running wheel activity in mice. PLoS ONE. 2017;12:e0184829.

85. Yu H, Wang DD, Wang Y, Liu T, Lee FS, Chen ZY. Variant brain-derived neurotrophic factor Val66Met polymorphism alters vulnerability to stress and response to antidepressants. J Neurosci. 2012;32:4092–101.

86. Yoon SH, Kim BH, Ye SK, Kim MH. Chronic non-social stress affects depressive behaviors but not anxiety in mice. Korean J Physiol Pharmacol. 2014;18:263–8.

87. Velligan DI, Diamond P, Glahn DC, Ritch J, Maples N, Castillo D, Miller AL. The reliability and validity of the Test of Adaptive Behavior in Schizophrenia (TABS). Psychiatry Res. 2007;151:55–66.

88. Pugliese CE, Anthony L, Strang JF, Dudley K, Wallace GL, Kenworthy L. Increasing adaptive behavior skill deficits from childhood to adolescence in autism spectrum disorder: role of executive function. J Autism Dev Disord. 2015;45:1579–87.

89. Matejcek Z. Is ADHD adaptive or non-adaptive behavior? Neuro Endocrinol Lett. 2003;24:148–50.

90. Stein MA, Szumowski E, Blondis TA, Roizen NJ. Adaptive skills dysfunction in ADD and ADHD children. J Child Psychol Psychiatry. 1995;36:663–70.

91. Matsumoto Y, Katayama K, Okamoto T, Yamada K, Takashima N, Nagao S, Aruga J. Impaired auditory-vestibular functions and behavioral abnormalities of Slitrk6-deficient mice. PLoS ONE. 2011;6:e16497.

92. Komada M, Takao K, Miyakawa T. Elevated plus maze for mice. J Vis Exp. 2008;22:22.

93. de Araújo Costa Folha OA, Bahia CP, de Aguiar GPS, Herculano AM, Coelho NLG, de Sousa MBC, Shiramizu VKM, de Menezes Galvão AC, de Carvalho WA, Pereira A. Effect of chronic stress during adolescence in prefrontal cortex structure and function. Behav Brain Res. 2017;326:44–51.

94. Burokas A, Martín-García E, Gutiérrez-Cuesta J, Rojas S, Herance JR, Gispert JD, Serra MÁ, Maldonado R. Relationships between serotonergic and cannabinoid system in depressive-like behavior: a PET study with [11C]-DASB. J Neurochem. 2014;130:126–35.

95. Yao B, Cheng Y, Wang Z, Li Y, Chen L, Huang L, Zhang W, Chen D, Wu H, Tang B, Jin P. DNA N6-methyladenine is dynamically regulated in the mouse brain following environmental stress. Nat Commun. 2017;8:1122.

96. Monteiro S, Roque S, de Sá-Calçada D, Sousa N, Correia-Neves M, Cerqueira JJ. An efficient chronic unpredictable stress protocol to induce stress-related responses in C57BL/6 mice. Front Psychiatry. 2015;6:6.

97. Miyata S, Koyama Y, Takemoto K, Yoshikawa K, Ishikawa T, Taniguchi M, Inoue K, Aoki M, Hori O, Katayama T, Tohyama M. Plasma corticosterone activates SGK1 and induces morphological changes in oligodendrocytes in corpus callosum. PLoS ONE. 2011;6:e19859.

98. Chu X, Zhou Y, Hu Z, Lou J, Song W, Li J, Liang X, Chen C, Wang S, Yang B, Chen L, Zhang X, Song J, Dong Y, Chen S, He L, Xie Q, Chen X, Li W. 24-hour-restraint stress induces long-term depressive-like phenotypes in mice. Sci Rep. 2016;6:32935.

99. Jeong JY, Lee DH, Kang SS. Effects of chronic restraint stress on body weight, food intake, and hypothalamic gene expressions in mice. Endocrinol Metab (Seoul). 2013;28:288–96.

100. Lyons DM, Parker KJ, Schatzberg AF. Animal models of early life stress: implications for understanding resilience. Dev Psychobiol. 2010;52:616–24.

101. Trainor BC, Pride MC, Villalon Landeros R, Knoblauch NW, Takahashi EY, Silva AL, Crean KK. Sex differences in social interaction behavior following social defeat stress in the monogamous California mouse (*Peromyscus californicus*). PLoS ONE. 2011;6:e17405.

102. Greenberg GD, Laman-Maharg A, Campi KL, Voigt H, Orr VN, Schaal L, Trainor BC. Sex differences in stress-induced social withdrawal: role of brain derived neurotrophic factor in the bed nucleus of the stria terminalis. Front Behav Neurosci. 2014;7:223.

103. Inan M, Zhao M, Manuszak M, Karakaya C, Rajadhyaksha AM, Pickel VM, Schwartz TH, Goldstein PA, Manfredi G. Energy deficit in parvalbumin neurons leads to circuit dysfunction, impaired sensory gating and social disability. Neurobiol Dis. 2016;93:35–46.

104. Li J, Li HX, Shou XJ, Xu XJ, Song TJ, Han SP, Zhang R, Han JS. Effects of chronic restraint stress on social behaviors and the number of hypothalamic oxytocin neurons in male rats. Neuropeptides. 2016;60:21–8.

105. Herman JP, Flak J, Jankord R. Chronic stress plasticity in the hypothalamic paraventricular nucleus. Prog Brain Res. 2008;170:353–64.

106. Brüne M, Schaub D, Juckel G, Langdon R. Social skills and behavioral problems in schizophrenia: the role of mental state attribution, neurocognition and clinical symptomatology. Psychiatry Res. 2011;190:9–17.

107. O'Haire ME, McKenzie SJ, Beck AM, Slaughter V. Social behaviors increase in children with autism in the presence of animals compared to toys. PLoS ONE. 2013;8:e57010.

108. Alessandri SM. Attention, play, and social behavior in ADHD preschoolers. J Abnorm Child Psychol. 1992;20:289–302.

109. Marín O. Interneuron dysfunction in psychiatric disorders. Nat Rev Neurosci. 2012;13:107–20.

110. Rossignol E. Genetics and function of neocortical GABAergic interneurons in neurodevelopmental disorders. Neural Plast. 2011;2011:649325.

111. Enwright JF III, Huo Z, Arion D, Corradi JP, Tseng G, Lewis DA. Transcriptome alterations of prefrontal cortical parvalbumin neurons in schizophrenia. Mol Psychiatry. 2017. https://doi.org/10.1038/mp.2017.216.

112. Paylor JW, Lins BR, Greba Q, Moen N, Moraes RS, Howland JG, Winship IR. Developmental disruption of perineuronal nets in the medial prefrontal cortex after maternal immune activation. Sci Rep. 2016;6:37580.

113. Jiao Y, Zhang Z, Zhang C, Wang X, Sakata K, Lu B, Sun QQ. A key mechanism underlying sensory experience-dependent maturation of neocortical GABAergic circuits in vivo. Proc Natl Acad Sci USA. 2011;108:12131–6.

114. Koh DX, Sng JC. HDAC1 negatively regulates Bdnf and Pvalb required for parvalbumin interneuron maturation in an experience-dependent manner. J Neurochem. 2016;139:369–80.

115. Chattopadhyaya B, Di Cristo G, Higashiyama H, Knott GW, Kuhlman SJ, Welker E, Huang ZJ. Experience and activity-dependent maturation of perisomatic GABAergic innervation in primary visual cortex during a postnatal critical period. J Neurosci. 2004;24:9598–611.

116. Ueno H, Suemitsu S, Okamoto M, Matsumoto Y, Ishihara T. Sensory experience-dependent formation of perineuronal nets and expression of Cat-315 immunoreactive components in the mouse somatosensory cortex. Neuroscience. 2017;355:161–74.

117. McRae PA, Porter BE. The perineuronal net component of the extracellular matrix in plasticity and epilepsy. Neurochem Int. 2012;61:963–72.

118. Yamada J, Ohgomori T, Jinno S. Perineuronal nets affect parvalbumin expression in GABAergic neurons of the mouse hippocampus. Eur J Neurosci. 2015;41:368–78.

119. Yoshioka N, Miyata S, Tamada A, Watanabe Y, Kawasaki A, Kitagawa H, Takao K, Miyakawa T, Takeuchi K, Igarashi M. Abnormalities in

Ueno *et al. BMC Neurosci (2018) 19:41*

Page 21 of 21

perineuronal nets and behavior in mice lacking CSGalNAcT1, a key enzyme in chondroitin sulfate synthesis. Mol. Brain. 2017;10:47.

120. Tottenham N, Sheridan MA. A review of adversity, the amygdala and the hippocampus: a consideration of developmental timing. Front Hum Neurosci. 2010;3:68.

121. Fenoglio KA, Brunson KL, Baram TZ. Hippocampal neuroplasticity induced by early-life stress: functional and molecular aspects. Front Neuroendocrinol. 2006;27:180–92.

122. Andersen SL, Teicher MH. Delayed effects of early stress on hippocampal development. Neuropsychopharmacology. 2004;29:1988–93.

123. Benes FM, Turtle M, Khan Y, Farol P. Myelination of a key relay zone in the hippocampal formation occurs in the human brain during childhood, adolescence, and adulthood. Arch Gen Psychiatry. 1994;51:477–84.

124. McEwen BS, Morrison JH. The brain on stress: vulnerability and plasticity of the prefrontal cortex over the life course. Neuron. 2013;79:16–29.

125. McEwen BS, Nasca C, Gray JD. Stress effects on neuronal structure: hippocampus, amygdala, and prefrontal cortex. Neuropsychopharmacology. 2016;41:3–23.

126. Weich S, Patterson J, Shaw R, Stewart-Brown S. Family relationships in childhood and common psychiatric disorders in later life: systematic review of prospective studies. Br J Psychiatry. 2009;194:392–8.

127. Kausch O, Rugle L, Rowland DY. Lifetime histories of trauma among pathological gamblers. Am J Addict. 2006;15:35–43.

128. de Pablos RM, Herrera AJ, Espinosa-Oliva AM, Sarmiento M, Muñoz MF, Machado A, Venero JL. Chronic stress enhances microglia activation and exacerbates death of nigral dopaminergic neurons under conditions of inflammation. J Neuroinflammation. 2014;11:34.